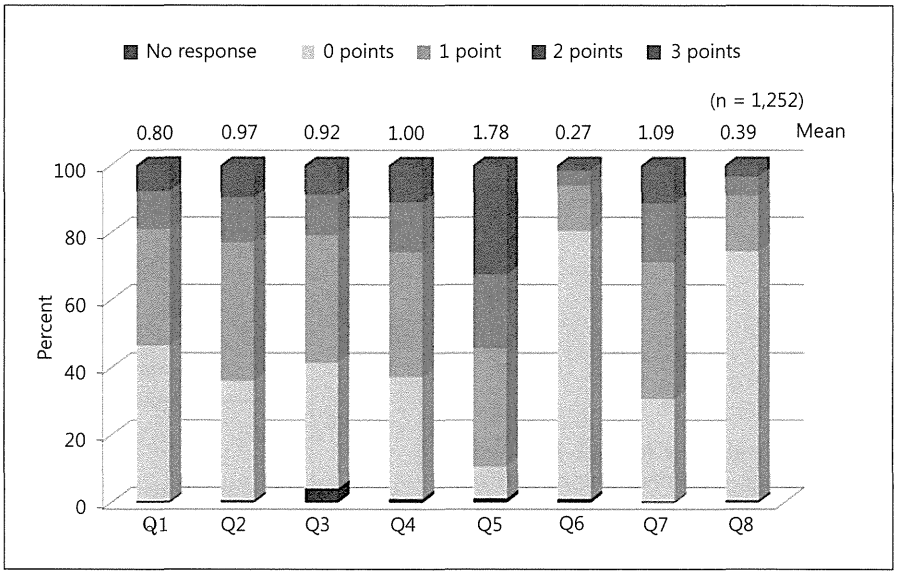

Fig. 1. Distribution of points for each JESS question. Chance of dozing in a given situation: Q1 = Sitting and reading; Q2 = watching TV; Q3 = sitting inactive in a public place (e.g. a theater or a meeting); Q4 = as passenger in a car for an hour without a break; Q5 = lying down to rest in the afternoon when circumstances permit; Q6 = sitting and talking to someone; Q7 = sitting quietly after a lunch without alcohol; Q8 = in a car, while stopped for a few minutes in traffic. 0 = No chance of dozing; 1 = slight chance of dozing; 2 = moderate chance of dozing; 3 = high chance of dozing.

Table 2. Association of JESS score groups and other variables on all-cause mortality

Variables	Univariate analysis			Multivariate analysis		
	HR	95% CI	p value	HR	95% CI	p value
JESS score (ref. low score)						
Intermediate score	1.427	0.808–2.518	0.220	1.131	0.627–2.040	0.684
High score	3.396	1.922–5.998	<0.001	**2.312**	**1.267–4.220**	**0.006**
Elderly group (≥70 years)	4.043	2.508–6.519	<0.001	**2.859**	**1.704–4.799**	**<0.001**
Vintage (per 1 year)	0.998	0.968–1.028	0.875	1.026	0.990–1.064	0.157
Male gender	1.175	0.753–1.832	0.477	1.555	0.942–2.568	0.085
Primary disease (DM)	1.496	0.959–2.334	0.076	1.035	0.616–1.738	0.896
Comorbidities						
Congestive heart failure	2.985	1.920–4.642	<0.001	**2.094**	**1.301–3.370**	**0.002**
Cancer (other than skin)	2.012	1.098–3.688	0.024	1.290	0.691–2.411	0.424
Hypertension	1.233	0.760–2.000	0.396	1.161	0.701–1.922	0.562
Lung disease	6.658	3.261–13.59	<0.001	**4.282**	**1.908–9.609**	**<0.001**
Neurologic disorder	2.352	1.394–3.967	0.001	1.642	0.910–2.961	0.100
CVD composite	2.149	1.383–3.342	<0.001	1.159	0.711–1.888	0.555
BMI (ref. Q1, <19.00)						
Q2 (19.00–20.99)	0.578	0.327–1.021	0.059	0.597	0.324–1.101	0.099
Q3 (21.00–22.99)	0.551	0.298–1.017	0.057	**0.487**	**0.240–0.987**	**0.046**
Q4 (≥23.00)	0.555	0.314–0.981	0.043	0.699	0.370–1.322	0.271
Albumin (ref. T1, <3.70 g/dl)						
T2 (3.70–3.99)	0.495	0.302–0.812	0.005	**0.595**	**0.356–0.994**	**0.047**
T3 (≥4.00)	0.286	0.159–0.515	<0.001	**0.388**	**0.209–0.719**	**0.003**
Dialysis time ≥240 min/session	0.713	0.436–1.165	0.177	0.843	0.464–1.532	0.576
Dialysis frequency (<3 times/week)	1.529	0.432–5.417	0.511	1.414	0.371–5.388	0.612
Single pool Kt/V ≥1.2	0.938	0.569–1.544	0.801	0.958	0.521–1.764	0.891
Erythropiesis-stimulating agent	1.057	0.599–1.865	0.849	0.899	0.490–1.648	0.731
Hypnotic agent	1.146	0.735–1.787	0.548	0.871	0.548–1.383	0.558

DM = Diabetes mellitus; T = tertile. Values set in boldface are significant.

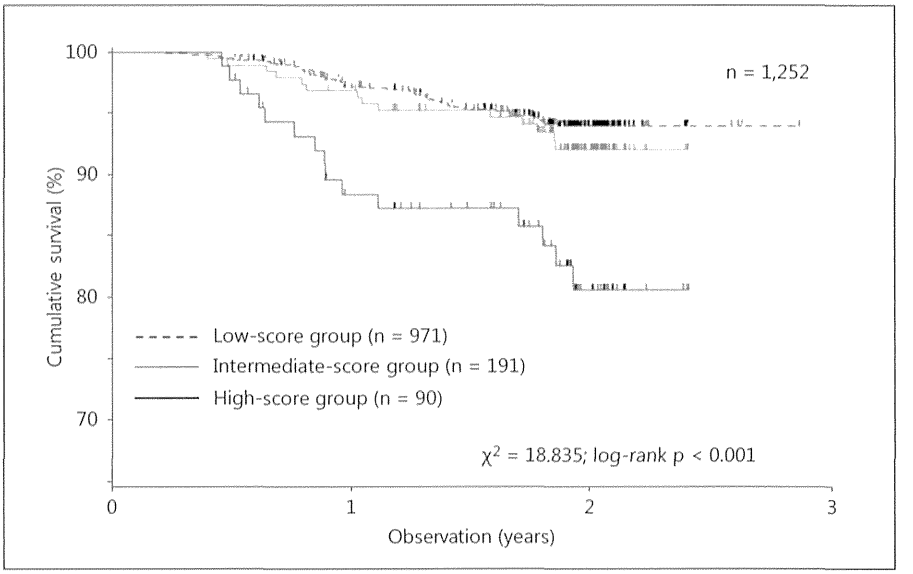

Fig. 2. Survival curve for each JESS score group by age. Patients were categorized into three subgroups: low (JESS score 0–10), intermediate (JESS score 11–15), and high (JESS score 16–24).

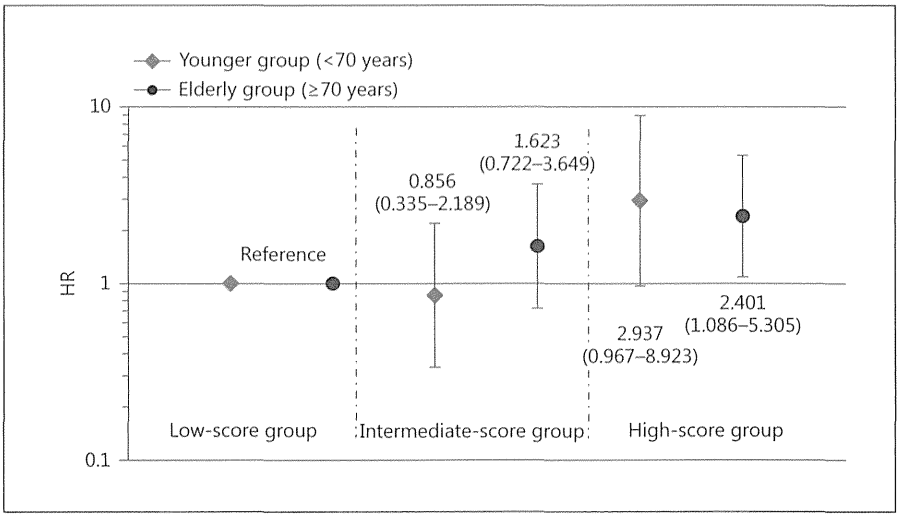

Fig. 3. Effect of JESS score on survival in younger and elderly patients. Patients were categorized into three subgroups: low (JESS score 0–10), intermediate (JESS score 11–15), and high (JESS score 16–24). Results of multi-imputation analysis were adjusted for age, vintage, sex, diabetics, comorbidities (congestive heart failure, cancer, hypertension, lung disease, neurologic disorder, and CVD composite), BMI, single-pool Kt/V, dialysis time, dialysis frequency, albumin, and erythropoiesis-stimulating agent prescription.

variables such as serum albumin, creatinine, and total cholesterol were significantly lower among those with high JESS scores.

Responses to each question of the JESS questionnaire are summarized in figure 1. We obtained more than 95% of responses for each question. The mean score was 0.89 (0.46 SD), ranging from 0.27 to 1.78. Among the questions, the JESS score was highest (1.78) for question number 5, 'While lying down and taking a rest in the afternoon'. It was lowest (0.27) for question number 6, 'While sitting and talking with someone'. The mean total JESS score was 7.13 (5.09 SD). There were 971 (77.6%) subjects who were grouped as low-risk, 191 (15.3%) as intermediate-risk, and 90 (7.2%) as high-risk.

Outcomes

During the study period, there were 85 deaths. The overall mortality rate was 36.4 per 1,000 patient-years. Causes of death were CVD in 32 (37.6%), malignancies in 13 (15.3%), infection in 12 (14.1%), miscellaneous in 5 (5.9%), and unknown in 23 (27.1%) patients. Cumulative survival rates of the three subgroups according to baseline JESS score are shown in figure 2. With higher JESS scores, survival was poor. The adjusted HR was 2.312 (95% CI 1.267–4.220; p = 0.006) compared to those with low JESS scores (table 2). Results of the Kaplan-Meier method with the log-rank test have been summarized for the younger group (age <70 years) and elderly group (age ≥70 years). The relative risk of death was significantly higher in high-

Table 3. Factors associated with high JESS score (≥16) and patients background

Variables	Univariate analysis			Multivariate analysis		
	OR	95% CI	p value	OR	95% CI	p value
Elderly group (≥70 years)	2.631	1.699–4.074	<0.001	**1.750**	**1.078–2.841**	**0.024**
Vintage, years	1.053	1.014–1.093	0.007	0.981	0.941–1.023	0.377
Primary disease (DM)	1.910	1.231–2.965	0.004	1.485	0.545–4.052	0.440
Comorbidities						
Congestive heart failure	1.724	1.047–2.837	0.032	1.241	0.731–2.105	0.424
Cerebrovascular disease	2.474	1.404–4.358	0.002	**1.969**	**1.079–3.592**	**0.027**
DM	1.841	1.193–2.842	0.006	0.849	0.308–2.341	0.752
Neurologic disorder	1.839	1.022–3.307	0.042	1.105	0.580–2.102	0.762
Creatinine (ref. Q1, <9.00 mg/dl)						
Q2 (9.00–10.99)	0.505	0.296–0.861	0.012	0.603	0.336–1.085	0.091
Q3 (11.00–12.99)	0.157	0.072–0.340	<0.001	**0.248**	**0.108–0.572**	**0.001**
Q4 (≥13.00)	0.340	0.188–0.614	<0.001	0.625	0.303–1.290	0.203
Hemoglobin (ref. Q1, <9.70 g/dl)						
Q2 (9.70–10.46)	0.562	0.307–1.028	0.062	0.655	0.351–1.223	0.184
Q3 (10.50–11.25)	0.669	0.372–1.202	0.178	0.841	0.454–1.558	0.582
Q4 (≥11.30)	0.612	0.332–1.127	0.115	0.863	0.444–1.676	0.663
Serum phosphorus (ref. T1, <4.77 mg/dl)						
T2 (4.80–5.89)	0.733	0.434–1.236	0.244	0.997	0.572–1.737	0.991
T3 (≥5.90)	0.679	0.403–1.143	0.145	1.022	0.575–1.817	0.941
Dialysis time ≥240 min/session	0.638	0.394–1.035	0.069	1.109	0.640–1.921	0.713
Phosphate binder (ref. no)						
Calcium based	0.507	0.303–0.849	0.010	0.768	0.439–1.346	0.357
Non-calcium based	0.511	0.253–1.032	0.061	1.077	0.486–2.386	0.856
Combined	0.232	0.093–0.579	0.002	0.503	0.184–1.375	0.181
Erythropiesis-stimulating agent	2.196	1.046–4.608	0.038	1.741	0.783–3.869	0.174

DM = Diabetes mellitus; T = tertile. Values set in boldface are significant.

scoring groups, even after multiple adjustments. Among patients aged ≥70 years, outcomes for the high-scoring JESS group were significantly worse when compared with the low-scoring JESS group [adjusted HR 2.401 (95% CI 1.086–5.305); p = 0.030; fig. 3]. There was no interaction between age and JESS score.

Factors Related to the High JESS Score

Elderly patients (≥70 years) with comorbid conditions such as cerebrovascular disease had significantly higher JESS scores (≥16). In the high-scoring JESS group, the serum creatinine level seemed to be rather low (table 3).

Discussion

We observed that high JESS scores predicted poor survival, particularly in elderly patients. Although the high JESS scores were associated with several clinical and laboratory factors (table 1), early detection of sleepiness would be beneficial for survival. The HD vintage was shorter among those with high JESS scores, possibly reflecting survival bias, as death rates are high in such patients. Phosphate binders and vitamin D derivatives were used less frequently among those with high JESS scores. We found a reported positive relation [14] between phosphate levels and SQ, restless legs syndrome, and survival, but others did not [15, 16]. The Japanese HD population had a higher prevalence of pruritus than that of the USA [17]. Pruritus, which has often been associated with hyperphosphatemia, was shown to increase odds of poor JESS scores [18, 19]. Hypercalcemia was associated with poor mental health in Japanese HD patients [19]. Others suggested an effect of depression and the use of benzodiazepines on survival [20].

The present study supports the notion that the JESS questionnaire is a reliable and valid tool to evaluate

sleep disorders and SQ for Japanese HD patients. Details of the modification, reliability, and validation were reported previously in a non-HD population [9]. Patients with higher JESS scores showed worse daytime function as measured with the Pittsburgh Sleep Quality Index. However, there might be further concerns regarding the translation and cultural adaptation of the questionnaire [21]. To our knowledge, this is the first application to chronic HD patients, in particular to aged HD patients. Accordingly, the present result is clinically relevant as the prevalence of elderly HD patients is close to 50% of the total patient population in Japan (www.jsdt.or.jp).

Daytime sleepiness may be related to the disturbance of the sleep-wake rhythm. The circadian rhythm of melatonin produced by the pineal gland is often blunted in dialysis patients [22]. Also, melatonin secretion is often decreased in chronic HD patients [23]. Exogenous melatonin may be effective in such cases. β-Blockers have also been shown to depress nocturnal production of melatonin. However, they are not often used in Japanese HD patients.

Sleep apnea syndrome is common in pre-HD and HD chronic kidney disease patients, and they often have CVDs. Obesity (BMI ≥25) is often associated with sleep apnea. However, obesity is rare among Japanese HD patients; therefore, a simple questionnaire like the JESS would be better motivated. Among the DOPPS countries, the mean SQ score was highest and the death risk was lowest in Japan [8]. Sleep disorders have been reported as a predictor of mortality in HD patients [24]. However, the number of subjects was small and the mortality rate was very high; the annual mortality rate was >20% [24]. The evidence that sleep disorders and sleep apnea induce CVD in end-stage renal disease remains circumstantial [25]. According to previous DOPPS papers, a longer HD treatment time, a relatively low blood flow rate, and a predominant use of native arteriovenous fistulae are characteristic in Japanese dialysis units [26]. However, the mortality rate is rather low despite higher levels of blood pressure and lower hemoglobin levels [27].

A limitation of our study is that SQ has not been validated among Japanese dialysis patients. However, we used a similar questionnaire concerning SQ [28–30]. The DOPPS does not collect data on the daytime and nighttime shift of dialysis. Most HD patients are lying in bed during HD sessions in Japan. Therefore, it is common for them to fall asleep during HD, as reported previously [31, 32]. Currently, more than 85% of the HD patients are dialyzed during the day. It is possible that a shift change in HD may change sleepiness [33]. We could not completely adjust for the impact of residual confounding variables [27, 34]. Daytime sleepiness may differ from sleepiness in the dark laboratory conditions used to measure the Multiple Sleep Latency Test (MSLT), and we did not confirm the presence of sleep apnea by polysomnogram [35, 36].

In conclusion, our results showed that the assessment of sleepiness by JESS scores is useful for identifying patients at risk of death among chronic HD patients, in particular aged patients. There was no interaction between age and JESS score. In patients with high JESS scores (≥16), lifestyle modifications such as exercise [37] and further evaluation of sleep disturbance would be warranted. Future studies are necessary to examine the causes of sleepiness and survival [38, 39] and the impact of treatment of sleepiness on survival. Mechanisms of adverse effects of sleepiness on survival are unknown. A better fluid clearance and attenuation of sympathetic activation would be expected by adequate sleep [40–42].

Acknowledgements

We wish to express appreciation to the steering committee members of J-DOPPS, Dr. Kiyoshi Kurokawa, Dr. Akira Saito, Dr. Tadao Akizawa, Dr. Takashi Akiba, and Dr. Shunichi Fukuhara. We are also grateful to the study nurses, physicians, and medical directors for all the time and attention they have devoted to our study. J-DOPPS was administered by the Arbor Research Collaborative for Health, Ann Arbor, Mich., USA, and supported by Kyowa-Hakko-Kirin Co., Ltd., without restriction on publication.

Disclosure Statement

K. Iseki, K. Tsuruya, E. Kanda, and H. Hirakata are on the advisory board of the Kyowa-Hakko Kirin.

References

1 Sivalingam M, Chakravorty I, Mouatt S, Farrington K: Obstructive sleep apnea in incremental hemodialysis: determinants, consequences, and impact on survival. Hemodial Int 2013;17:230–239.
2 Sakkas GK, Gourgoulianis KI, Karatzaferi C, et al: Haemodialysis patients with sleep apnoea syndrome experience increased central adiposity and altered muscular composition and functionality. Nephrol Dial Transplant 2008;23:336–344.
3 Kuhlmann U, Becker HF, Birkhahn M, et al: Sleep-apnea in patients with end-stage renal disease and objective results. Clin Nephrol 2000;53:460–466.

4 Iseki K: Role of chronic kidney disease in cardiovascular disease: are we different from others? Clin Exp Nephrol 2011;15:450–455.
5 Unruh ML, Hartunian MG, Chapman MM, Jaber BL: Sleep quality and clinical correlates in patients on maintenance dialysis. Clin Nephrol 2003;59:280–288.
6 Young EW, Goodkin D, Mapes DM, et al: The Dialysis Outcomes and Practice Patterns Study (DOPPS): an international hemodialysis study. Kidney Int 2000;57:S74–S81.
7 Pisoni RL, Gillespie BW, Dickinson DM, et al: The Dialysis Outcomes and Practice Patterns Study (DOPPS): design, data elements, and methodology. Am J Kidney Dis 2004;44:7–15.
8 Elder SJ, Pisoni RL, Akizawa T, et al: Sleep quality predicts quality of life and mortality risk in haemodialysis patients: results from the Dialysis Outcomes and Practice Patterns Study (DOPPS). Nephrol Dial Transplant 2008;23:998–1004.
9 Takegami M, Suzukamo Y, Wakita T, et al: Development of a Japanese version of the Epworth Sleepiness Scale (JESS) based on item response theory. Sleep Med 2009;10:556–565.
10 Johns MW: A new method for measuring daytime sleepiness: the Epworth Sleepiness Scale. Sleep 1991;14:540–545.
11 Johns MW: Reliability and factor analysis of the Epworth Sleepiness Scale. Sleep 1992;15:376–381.
12 Schafer JL: Analysis of Incomplete Multivariate Data. London, Chapman & Hall, 1997.
13 Rubin DB: Multiple Imputation for Nonresponse in Surveys. New York, Wiley, 1987.
14 Unruh ML, Hartunian MG, Chapman MM, et al: Sleep quality and clinical correlates in patients on maintenance dialysis. Clin Nephrol 2003;59:280–288.
15 Collado-Seidel V, Kohnen R, Samtleben W, et al: Clinical and biochemical findings in uremic patients with and without restless legs syndrome. Am J Kidney Dis 1998;31:324–328.
16 Huiqi Q, Shan L, Mingcai Q: Restless legs syndrome (RLS) in uremic patients is related to the frequency of hemodialysis sessions. Nephron 2000;86:540.
17 Pisoni RL, Wikstrom B, Elder SJ, et al: Pruritus in haemodialysis patients: international results from the Dialysis Outcomes and Practice Patterns Study (DOPPS). Nephrol Dial Transplant 2006;21:3495–3505.
18 Wikstrom B: Itchy skin – a clinical problem for haemodialysis patients. Nephrol Dial Transplant 2007;22(suppl 5):v3–v7.
19 Tanaka M, Yamazaki S, Hayashino Y, et al: Hypercalcemia is associated with poor mental health in haemodialysis patients: results from Japan DOPPS. Nephrol Dial Transplant 2007;22:1658–1664.
20 Fukuhara S, Green J, Albert J, et al: Symptoms of depression, prescription of benzodiazepines, and the risk of death in hemodialysis patients in Japan. Kidney Int 2006;70:1866–1872.
21 Green J, Fukuhara S, Shinzato T, et al: Translation, cultural adaptation, and initial reliability and multitrial testing of the Kidney Disease Quality of Life instrument for use in Japan. Qual Life Res 2001;10:93–100.
22 Koch BCP, Nagtegaal E, Hagen EC, et al: The effects of melatonin on sleep-wake rhythm of daytime haemodialysis patients: a randomized, placebo-controlled, cross-over study (EMSCAP study). Br J Clin Pharmacology 2009;67:68–75.
23 Karasek M, Szuflet A, Chrzanowski W, et al: Decreased melatonin nocturnal concentrations in hemodialyzed patients. Neuroendocrinol Lett 2005;26:653–656.
24 Benz RL, Pressman MR, Hovick ET, Peterson DD: Potential novel predictors of mortality in end-stage renal disease patients with sleep disorders. Am J Kidney Dis 2000;35:1052–1060.
25 Zoccali C, Mallamaci F, Tripepi G: Sleep apnea in renal patients. J Am Soc Nephrol 2001;12:2854–2859.
26 Kuriyama S: Characteristics of the clinical practice patterns of hemodialysis in Japan in consideration of DOPPS and the NKF/DOQI guidelines. Clin Exp Nephrol 2008;12:165–170.
27 Goodkin DA, Bragg-Gresham JL, Koenig KG, et al: Association of comorbid conditions and mortality in hemodialysis patients in Europe, Japan, and the United States: the Dialysis Outcomes and Practice Patterns Study (DOPPS). J Am Soc Nephrol 2003;14:3270–3277.
28 Unruh ML, Buysse DJ, Dew MA, et al: Sleep quality and its correlates in the first year of dialysis. Clin J Am Soc Nephrol 2006;1:802–810.
29 Buysse DJ, Reynolds CF 3rd, Monk TH, et al: The Pittsburgh Sleep Quality Index: a new instrument for psychiatric practice and research. Psychiatry Res 1989;28:193–213.
30 Netzer NC, Stoohs RA, Netzer CM, et al: Using the Berlin questionnaire to identify patients at risk for the sleep apnea syndrome. Ann Intern Med 1999;131:485–491.
31 Parker KP, Bliwise DL, Rye DB, De A: Intradialytic subjective sleepiness and oral body temperature. Sleep 2000;23:887–891.
32 Kutner N, Zhang R, Johansen K, Bliwise D: Associations among nocturnal sleep, daytime intradialytic sleep, and mortality risk in patients on daytime conventional hemodialysis: US Renal Data System special study data. Hemodial Int 2013;17:223–229.
33 Hanly PJ, Gabor JY, Chen C, Pierratos A: Daytime sleepiness in patients with CRF: impact of nocturnal hemodialysis. Am J Kidney Dis 2003;41:403–410.
34 Hayashino Y, Yamazaki S, Takegami M, et al: Association between number of comorbid conditions, depression, and sleep quality using the Pittsburgh Sleep Quality Index: results from a population-based survey. Sleep Med 2010;11:366–371.
35 Iseki K, Tohyama K, Matsumoto T, Nakamura H: High prevalence of chronic kidney disease among patients with sleep-related breathing disorder (SRBD). Hypertens Res 2008;31:249–255.
36 Nakamura H, Kanemura T, Takara C, et al: A retrospective analysis of 4,000 patients with OSA in Okinawa, Japan. Sleep Biol Rhythms 2009;7:103–112.
37 Tentori F, Elder SJ, Thumma J, et al: Physical exercise among participants in the Dialysis Outcomes and Practice Patterns Study (DOPPS): correlates and associated outcomes. Nephrol Dial Transplant 2010;25:3050–3062.
38 Masuda T, Murata M, Honma S, et al: Sleep-disordered breathing predicts cardiovascular events and mortality in hemodialysis patients. Nephrol Dial Transplant 2011;26:2289–2295.
39 Argekar P, Griffin V, Litaker D, Rahman M: Sleep apnea in hemodialysis patients: risk factors and effect on survival. Hemodial Int 2007;11:435–441.
40 Chan CT, Hanly P, Gabor J, et al: Impact of nocturnal hemodialysis on the variability of heart rate and duration of hypoxemia during sleep. Kidney Int 2004;65:661–665.
41 Hanly PJ, Pierratos A: Improvement of sleep apnea in patients with chronic renal failure who undergo nocturnal hemodialysis. N Engl J Med 2001;344:102–107.
42 Pierratos A: Nocturnal home hemodialysis: an update on a 5-year experience. Nephrol Dial Transplant 1999;14:2835–2840.

Renal denervation has blood pressure–independent protective effects on kidney and heart in a rat model of chronic kidney disease

Masahiro Eriguchi[1], Kazuhiko Tsuruya[1,2], Naoki Haruyama[1], Shunsuke Yamada[1], Shigeru Tanaka[1], Takaichi Suehiro[1], Hideko Noguchi[1], Kosuke Masutani[1], Kumiko Torisu[1] and Takanari Kitazono[1]

[1]*Department of Medicine and Clinical Science, Graduate School of Medical Sciences, Kyushu University, Fukuoka, Japan and* [2]*Department of Integrated Therapy for Chronic Kidney Disease, Graduate School of Medical Sciences, Kyushu University, Fukuoka, Japan*

We elucidate the underlying mechanisms of bidirectional cardiorenal interaction, focusing on the sympathetic nerve driving disruption of the local renin–angiotensin system (RAS). A rat model of N^{ω}-nitro-L-arginine methyl ester (L-NAME; a nitric oxide synthase inhibitor) administration was used to induce damage in the heart and kidney, similar to cardiorenal syndrome. L-NAME induced sympathetic nerve–RAS overactivity and cardiorenal injury accompanied by local RAS elevations. These were suppressed by bilateral renal denervation, but not by hydralazine treatment, despite the blood pressure being kept the same between the two groups. Although L-NAME induced angiotensinogen (AGT) protein augmentation in both organs, AGT mRNA decreased in the kidney and increased in the heart in a contradictory manner. Immunostaining for AGT suggested that renal denervation suppressed AGT onsite generation from activated resident macrophages of the heart and circulating AGT excretion from glomeruli of the kidney. We also examined rats treated with L-NAME plus unilateral denervation to confirm direct sympathetic regulation of intrarenal RAS. The levels of urinary AGT and renal angiotensin II content and the degrees of renal injury from denervated kidneys were less than those from contralateral innervated kidneys within the same rats. Thus, renal denervation has blood pressure–independent beneficial effects associated with local RAS inhibition.

Kidney International (2015) **87,** 116–127; doi:10.1038/ki.2014.220; published online 18 June 2014

KEYWORDS: angiotensin; chronic kidney disease; fibrosis; renin–angiotensin system; renal ablation

Correspondence: *Kazuhiko Tsuruya, Department of Integrated Therapy for Chronic Kidney Disease, Graduate School of Medical Sciences, Kyushu University, 3-1-1 Maidashi, Fukuoka, Higashi-ku 812-8582, Japan. E-mail: tsuruya@intmed2.med.kyushu-u.ac.jp*

Received 11 January 2014; revised 5 May 2014; accepted 8 May 2014; published online 18 June 2014

Chronic kidney disease (CKD) may lead to heart failure and is associated with high mortality,[1] and heart failure may lead to renal failure.[2] Cardiac and renal dysfunction amplifies the failure of the other organ in acute and/or chronic situations. A new classification[3] was proposed to help the 'clinical' understanding of heart and kidney interactions, but understanding of the 'biological' mechanisms of this interaction remains limited. The sympathetic nervous system, the renin–angiotensin system (RAS), and nitric oxide (NO) are thought to have key roles in the cardiorenal cycle.[4] To investigate sympathetic nerve–RAS interaction, we developed a cardiorenal syndrome model with induced chronic NO depletion.

Although several clinical studies have reported the potential efficacies of renal sympathetic denervation (DNx) for resistant hypertension,[5] left ventricular hypertrophy,[6] albuminuria,[7] glucose metabolism,[8] sleep apnea syndrome,[9] arterial stiffness,[10] and CKD,[11] most studies were uncontrolled. A recent study, the SYMPLICITY-HTN-3 trial, was a blinded, randomized sham-controlled trial and failed to show any benefit of catheter-based DNx.[12] Currently, the underlying mechanisms are unclear and information on the procedure is limited.[13] Many clinicians think the clinically refractory nature of cardiorenal syndrome is an attractive target for intervention. The current study examined the beneficial effects of DNx on the sympathetic cross-talk with RAS in cardiorenal syndrome, with a focus on local RAS in the heart and kidney.

Local RAS has paracrine and intracrine roles independent of circulating RAS, and have been extensively reviewed.[14–17] Physiologically, intrarenal RAS regulates the glomerular filtration rate,[18] blood pressure, and proximal tubular reabsorption.[19] Brain RAS modulates drinking behavior[20] and blood pressure.[21] Cardiac RAS has inotropic and chronotropic effects.[22] Pathophysiologically, a long-term elevation in local RAS leads to organ dysfunction: for example, hypertension and progression of CKD in the kidney,[23–25] hypertension in the brain,[26] cardiac hypertrophy, fibrosis, and remodeling in the heart.[27] Despite vast amounts of research on the local regulation of RAS, its mechanisms remain controversial.[28–31] This study also addressed the

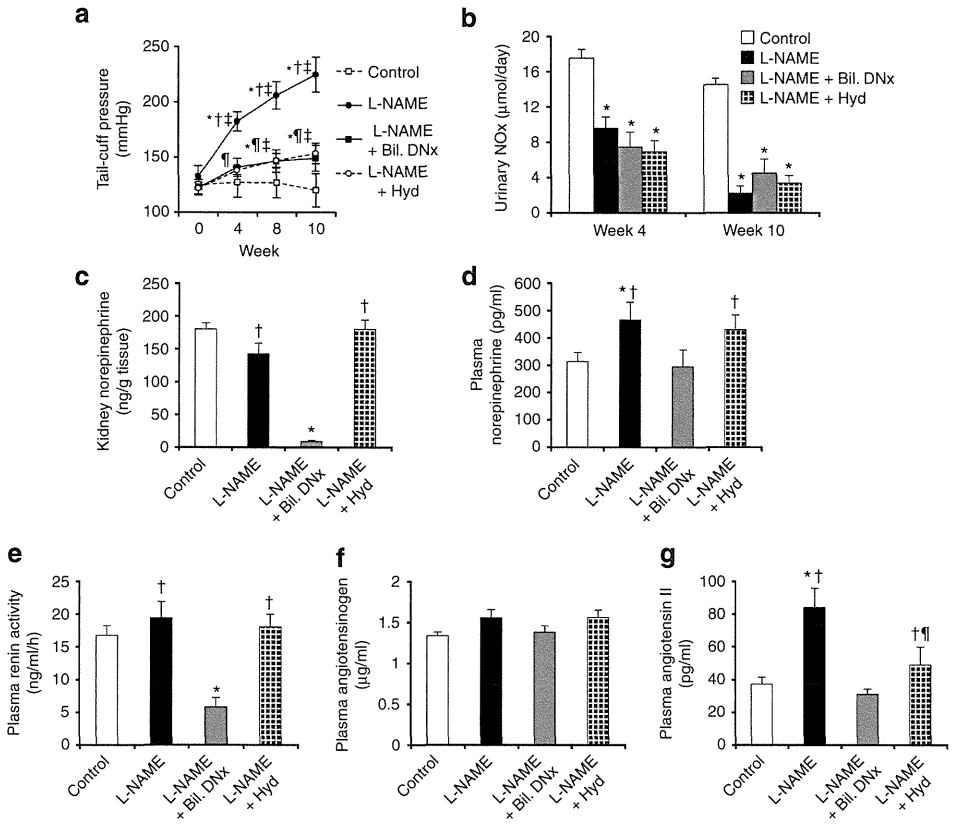

Figure 1 | The validity of renal denervation, blood pressure, and circulating factors in protocol 1. (**a**) Serial measurements of tail-cuff pressure. (**b**) Urinary nitrate/nitrite. Nitric oxide metabolite (NOx) levels at weeks 4 and 10 were equally suppressed among the three groups. (**c**) Renal cortical norepinephrine content levels were measured to confirm the validity of renal denervation. (**d**) Plasma norepinephrine and (**e**–**g**) RAS components were measured at the end of the study (week 10). Values are mean ± s.e.m. $^{*}P<0.05$ vs. control rats, $^{\dagger}P<0.05$ vs. Bil. DNx rats, $^{\P}P<0.05$ vs. L-NAME rats, $^{\ddagger}P<0.05$ vs. baseline values (week 0). Bil. DNx, bilateral renal denervation; L-NAME; N^{ω}-nitro-L-arginine methyl ester.

currently highly debated issue of the origin (tubular origin[31] or leakage from glomeruli[30]) of intrarenal angiotensinogen (AGT).

RESULTS

Renal denervation drives blood pressure-independent cardiorenal protection

We employed a cardiorenal syndrome model with NO depletion, which induced CKD and heart failure and bidirectional interaction between both damaged organs. In protocol 1, chronic N^{ω}-nitro-L-arginine methyl ester (L-NAME) administration induced a progressive elevation in tail-cuff pressure that reached approximately 220 mmHg over 10 weeks, and also showed lower body weights and hypoalbuminemia at the end of the study compared with other groups (Supplementary Table S1 online). Bilateral renal denervation (Bil. DNx) ameliorated the severe hypertension induced by L-NAME, resulting in tail-cuff pressure of approximately 150 mmHg at week 10. Tail-cuff pressures in rats treated with L-NAME and hydralazine were comparable to those in Bil. DNx rats (Figure 1a). These differences among L-NAME-treated groups were observed despite equal suppression of urinary and tissue NO metabolite production (Figure 1b and Supplementary Table S1 online). DNx was confirmed by a marked decrease in norepinephrine content in the denervated kidney at week 10 (Figure 1c). Systemic sympathetic nerve activity was inferred from plasma and urinary norepinephrine levels at week 10 (Figure 1d and Supplementary Table S1 online). These elevations were suppressed by Bil. DNx, but not by hydralazine (Figure 1d). Plasma renin activity was markedly suppressed in Bil. DNx rats compared with the other groups (Figure 1e). Plasma angiotensin II (AII) levels were higher in L-NAME- or hydralazine-treated rats compared with control or Bil. DNx rats (Figure 1g). There were no significant differences in plasma AGT levels, liver AGT protein, or mRNA levels among the groups (Figure 1f and Supplementary Figure S1 online). L-NAME administration induced severe proteinuria, glomerulosclerosis, and interstitial fibrosis (Figure 2a–e) and elevation in serum creatinine and blood urea nitrogen levels (Supplementary Table S1 online). Treatment with Bil. DNx, but not with hydralazine, suppressed all these changes in the kidney (Figure 2a–e), despite blood pressure being the same between these two groups (Figure 1a). L-NAME administration also induced cardiac hypertrophy, fibrosis, and systolic dysfunction. L-NAME-treated rats showed increased heart weight corrected by body weight (Figure 3a) and had left ventricular hypertrophy accompanied by cardiac fibrosis

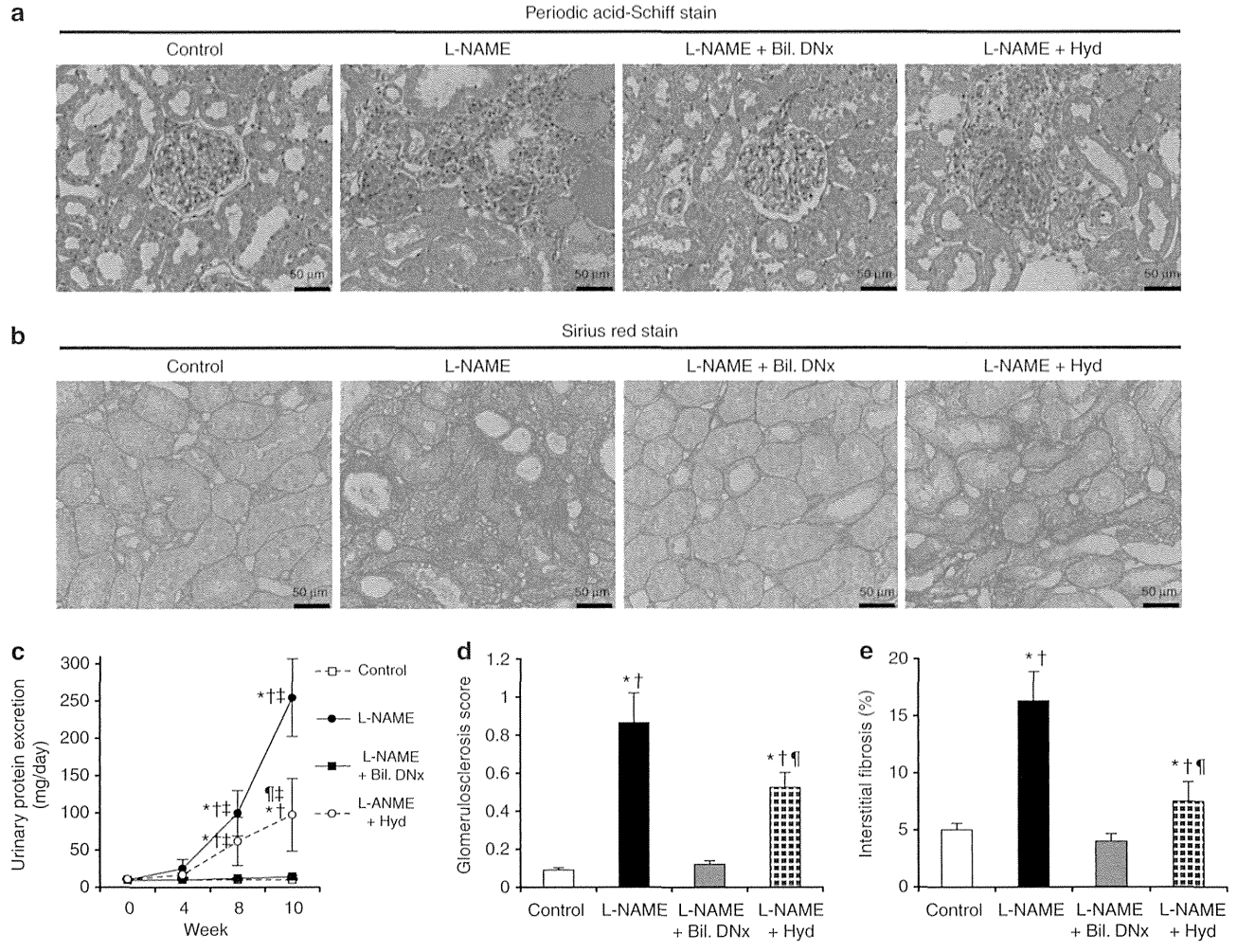

Figure 2 | Renal histological changes and proteinuria in protocol 1. Representative images using (**a**) Periodic acid-Schiff stain and (**b**) Sirius red stain (original magnification ×200). (**c**) Serial changes in proteinuria from 24-h urine collection. (**d**) The glomerulosclerosis index was assessed as previously described.[38,39] (**e**) Interstitial fibrosis using a point-counting technique.[38,39] Values are mean ± s.e.m. $^{*}P<0.05$ vs. control rats, $^{\dagger}P<0.05$ vs. Bil. DNx rats, $^{\P}P<0.05$ vs. L-NAME rats, $^{\ddagger}P<0.05$ vs. baseline values (week 0). Bil. DNx, bilateral renal denervation; L-NAME; N^{ω}-nitro-L-arginine methyl ester.

(Figure 3b; pale blue stain at interior side of left ventricle). Sirius red–stained representative images at high magnification are shown in Figure 3c. In echocardiography (Supplementary Table S2 online), L-NAME-treated rats exhibited increased left ventricular masses, left ventricular diastolic dimension dilation, left ventricular wall thickening that was expected from concentric hypertrophy (Figure 3d), and systolic dysfunction (Figure 3e). L-NAME administration also increased plasma brain natriuretic peptide and mRNA expression of brain natriuretic peptide in the left ventricle (Figure 3f and Supplementary Figure S3a online). Hydralazine treatment partially attenuated all changes related to cardiac injury that were suppressed to almost normal levels by Bil. DNx.

Renal denervation ameliorated local RAS in the heart and kidney

We investigated the local RAS components of heart and kidney tissues in protocol 1. L-NAME-treated rats showed progressive increases in urinary AGT, a feasible biomarker of intrarenal RAS.[15,32] Treatment with Bil. DNx suppressed these increases at levels comparable to those of control rats, but hydralazine treatment did not (Figure 4a). Western blot analyses (Figure 4b and c) revealed that renal cortical AGT protein levels were augmented in L-NAME-treated rats. We confirmed that renal cortical AII levels were significantly elevated in L-NAME-treated rats compared with control rats. Bil. DNx, but not hydralazine treatment, prevented elevations in cortical AII content (Figure 4d). Immunostaining for AGT to determine distribution in the kidney showed a faintly stained blush border of proximal tubules in control and Bil. DNx-treated rats. In contrast, rats treated with L-NAME or hydralazine showed strong staining of proximal tubules reaching the basal membrane and some glomerulus (Figure 4e).

Immunohistochemistry of cardiac tissue showed that AGT was expressed at void spaces of desmin-labeled myocytes consisting of normal cardiac interstitial spaces in control and

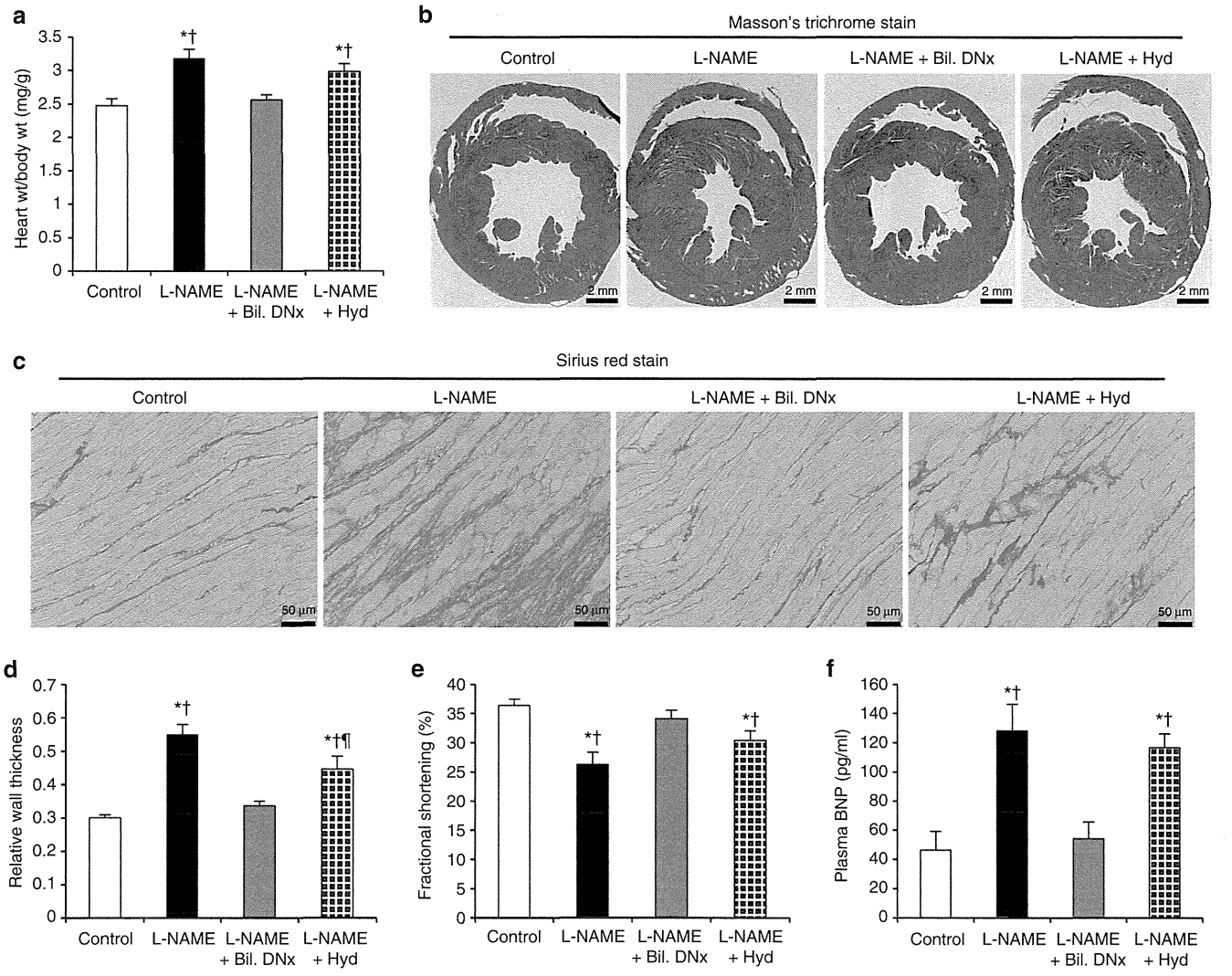

Figure 3 | Histological and functional changes of the heart in protocol 1. (**a**) Heart weight divided by body weight. (**b**) Representative images using Masson's trichrome stain (original magnification ×5). (**c**) Representative images using Sirius red stain (original magnification ×200). (**d**) Relative wall thickness [(AWTd + PWTd)/LVDd] and (**e**) fractional shortening measured by echocardiography. (**f**) Plasma brain natriuretic peptide levels measured at week 10. Values are mean ± s.e.m. $^{*}P<0.05$ vs. control rats, $^{\dagger}P<0.05$ vs. Bil. DNx rats, $^{\P}P<0.05$ vs. L-NAME rats. AWTd, anterior wall thickness in diastole; Bil. DNx, bilateral renal denervation; BNP, brain natriuretic peptide; L-NAME; N^{ω}-nitro-L-arginine methyl ester; LVDd, left ventricular dimension in diastole; PWTd, posterior wall thickness in diastole; wt, weight.

Bil. DNx rats, or pathological inflammatory/profibrotic lesions in L-NAME- and hydralazine-treated rats (Figure 5a). AGT (Figure 5b and c) and AII (Figure 5d) protein levels in the left ventricle were significantly higher in L-NAME-treated rats compared with control rats. These changes were suppressed by Bil. DNx, but not by hydralazine, treatment.

To examine the 'onsite generation' of local RAS components, we analyzed mRNA expression by RT–PCR. Tissue renin and angiotensin-converting enzyme (ACE) mRNA expression increased with L-NAME administration in both the left ventricle and renal cortex, and treatment with Bil. DNx normalized elevations in these mRNA expressions, but hydralazine treatment had limited effect (Figure 6a, b, d, and e). Interestingly, despite AGT protein augmentation in both the left ventricle and renal cortical tissue, AGT mRNA in each tissue was regulated in a contradictory manner: an upregulation of AGT mRNA in the left ventricle and a downregulation in the renal cortex (Figure 6c and f). These changes were also observed in AII type 1a receptor (Supplementary Figure S2a and S3b online). Increases in local RAS components in both organs induced elevation of profibrotic mRNA expression. Bil. DNx, but not hydralazine, treatment ameliorated these changes (Supplementary Figure S2b–e and S3c–f online).

Exploring the origin of locally regulated AGT protein in the heart and kidney

To clarify how local RAS components are regulated in each organ, we examined the origin of tissue AGT protein. In protocol 1, L-NAME administration amplified renal cortical AGT protein levels, despite the contradictory downregulation

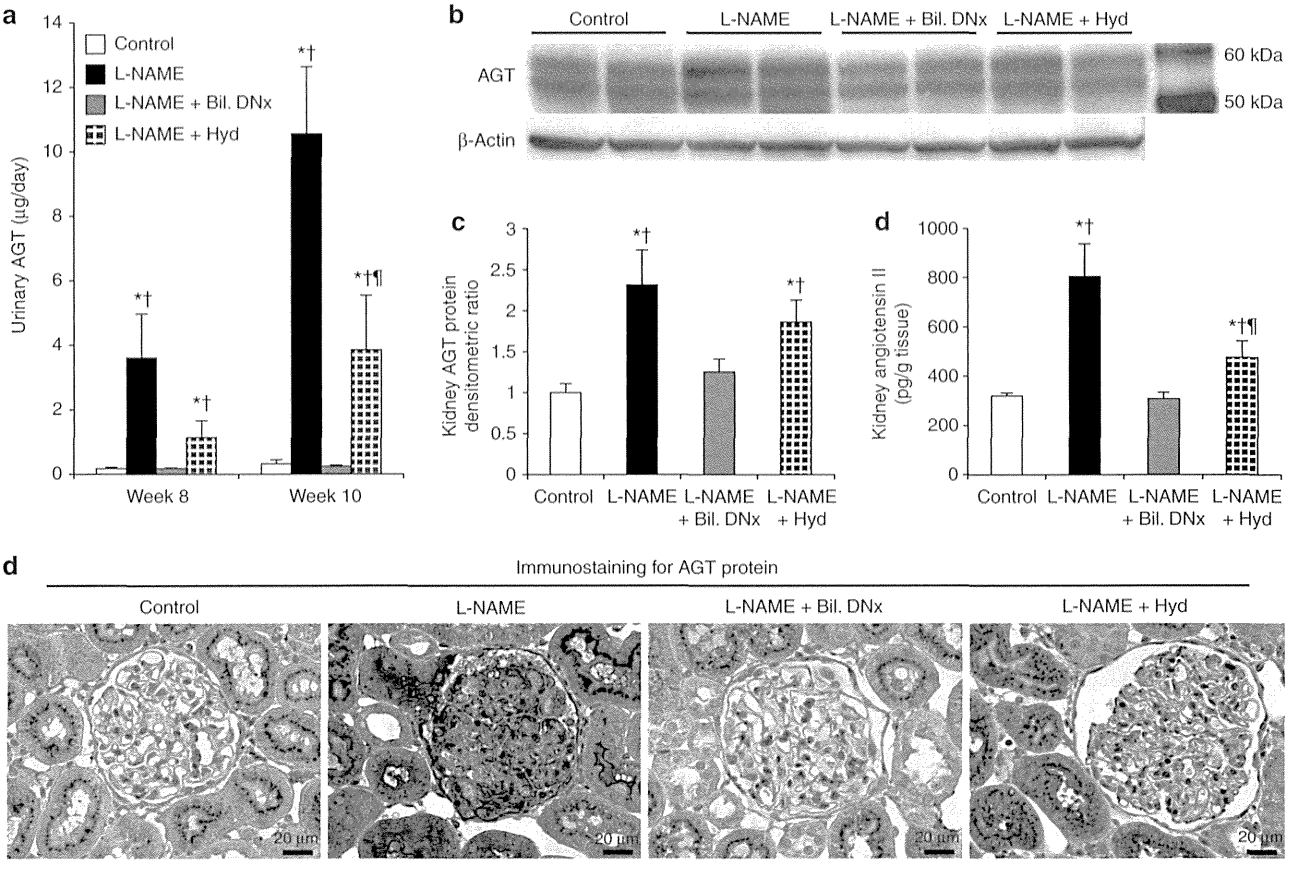

Figure 4 | Local renin–angiotensin system (RAS) components in the kidney in protocol 1. (**a**) Urinary AGT excretion at week 8 and 10. (**b**, **c**) AGT protein expression in renal cortical tissue using western blot analysis. (**b**) Two bands (59 kDa and 54 kDa) were detected, and (**c**) densitometric analysis was performed by sum of two differently glycosylated AGT bands ($n = 8$). (**d**) Renal cortical angiotensin II content levels. (**e**) Representative images of AGT immunostaining (original magnification ×400). Values are mean ± s.e.m. $^{*}P < 0.05$ vs. control rats, $^{\dagger}P < 0.05$ vs. Bil. DNx rats, $^{\P}P < 0.05$ vs. L-NAME rats. AGT, angiotensinogen; Bil. DNx, bilateral renal denervation; L-NAME; N^{ω}-nitro-L-arginine methyl ester.

of AGT mRNA expression. Immunostained images (Figure 7a and b) suggested that L-NAME administration induced AGT protein excretion through synaptopodin-labeled podocytes and desmin-labeled podocytes/mesangial cells; this change was suppressed by Bil. DNx. We then analyzed factors that affect urinary AGT. Urinary AGT was a feasible indicator of renal cortical AII ($R^2 = 0.82$; Figure 7c), as previously described.[32] Urinary protein excretion as a marker of glomerular permeability disorder had a strong positive association with urinary AGT levels ($R^2 = 0.96$; Figure 7d). In contrast, renal cortical AGT mRNA expression levels were negatively associated with urinary AGT levels ($R^2 = 0.25$; Figure 7e). These results suggest that filtrated circulating AGT was the precursor of renal cortical AII, and renal denervation might ameliorate glomerular AGT permeability.

In the left ventricle with a normal AGT regulatory condition, cardiac fibroblasts that were spindle-shaped vimentin-positive cells in the cardiac interstitial space rarely expressed AGT signals (Figure 7f(i) and f(ii)). Other vimentin-positive cardiac interstitial cells (macrophages, vascular smooth muscle cells, and pericytes) did not express AGT signals (Figure 7f(iii) and f(iv)). L-NAME induced proliferations of vimentin-positive cells in pathological interstitial lesions (Figure 7g(ii)), including cardiac fibroblasts, macrophages, vascular smooth muscle cells, pericytes, and α-smooth muscle actin (SMA)–positive activated cardiac fibroblast (so-called 'myofibroblast').

In the early phase of inflammatory lesions, strong AGT signals were expressed, and many cardiac fibroblasts, especially ED-1-labeled monocyte/macrophages, that produced AGT were seen (Figure 7g(i)-g(iii)). In contrast, in the late phase of fibrogenic lesions there were many α-SMA-positive cells, including myofibroblasts, pericytes, and vascular smooth muscle cells, with weak AGT deposition (Figure 7g(iv)). Renal denervation ameliorated local production of AGT in left ventricle tissue by abolishing infiltration of AGT-producing cardiac fibroblasts or macrophages, and suppressed myofibroblast proliferation as a result of the transformation of activated cardiac fibroblasts (Figure 7f).

Renal sympathetic nerves directly regulate intrarenal RAS

In protocol 1, Bil. DNx attenuated plasma RAS levels. This is reported to affect intrarenal RAS.[15,33] To confirm direct intrarenal RAS modulation by renal denervation, we observed rats treated with L-NAME + unilateral DNx and examined the laterality between the two kidneys of rats in

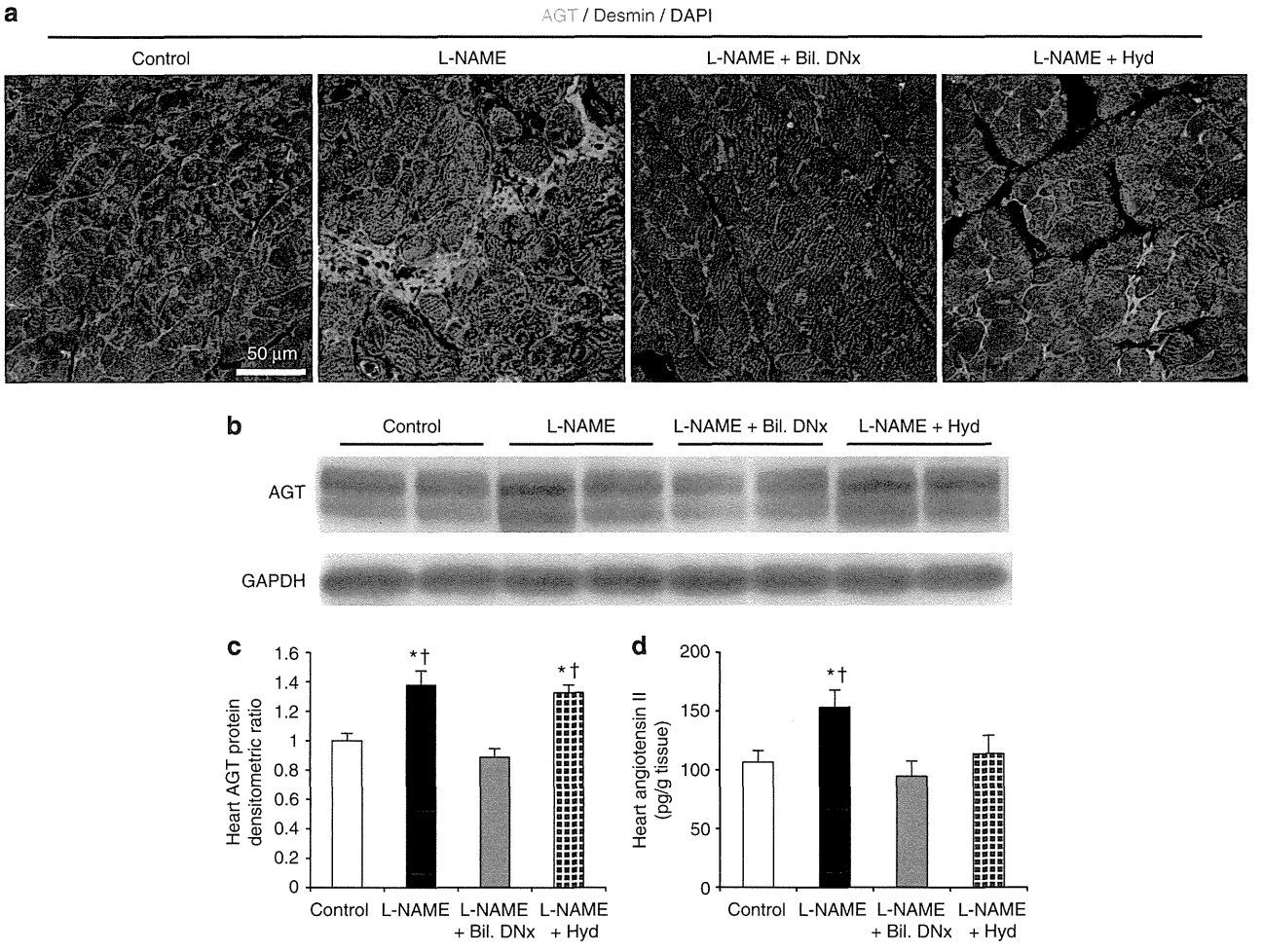

Figure 5 | Local renin–angiotensin system (RAS) components in the heart in protocol 1. (**a**) Representative images of AGT and desmin immunostaining from left ventricle (original magnification ×400; oil). (**b**, **c**) AGT protein expression in the left ventricle using western blot analysis. (**b**) Two bands (59 and 54 kDa) were detected, and (**c**) densitometric analysis was performed by the sum of two differently glycosylated AGT bands ($n = 8$). (**d**) Left ventricular angiotensin II content levels. Values are mean ± s.e.m. $^{*}P < 0.05$ vs. control rats, $^{\dagger}P < 0.05$ vs. Bil. DNx rats. AGT, angiotensinogen; Bil. DNx, bilateral renal denervation; DAPI, 4′,6-diamidino-2-phenylindole; GAPDH, glyceraldehyde-3-phosphate dehydrogenase; L-NAME; N^{ω}-nitro-L-arginine methyl ester.

protocol 2. First, we confirmed the validity of the findings that unilateral DNx and norepinephrine content levels of DNx kidneys were suppressed throughout the study (Figure 8a). In contrast to Bil. DNx treatment, unilateral DNx treatment could not suppress elevations in blood pressure, systemic sympathetic nervous activity, and RAS, and resulted in progressive renal failure (Supplementary Table S3 online).

Figure 8b and c show serial changes in intrarenal RAS between denervated (DNx) and contralateral innervated (non-DNx) kidneys. Urinary AGT excretion and cortical AII content levels of DNx kidneys were significantly or slightly lower than those of non-DNx kidneys at weeks 4, 8, and 10. Serial changes in renal cortical mRNA expression demonstrated that DNx kidneys had significantly lower expression of renin mRNA compared with non-DNx kidneys (Figure 8d). In contrast, AGT and ACE mRNA levels of DNx kidneys tended to be higher compared with those of non-DNx kidneys. As with protocol 1, AGT mRNA expression tended to decrease inversely over time, despite gradual increases in urinary AGT (Figure 8e and f).

Proteinuria excretion increased gradually with chronic administration of L-NAME, but proteinuria levels in DNx kidneys remained low up to week 8 and were significantly lower than those of non-DNx kidneys. These differences diminished at week 10 (Figure 8g). Histological examination showed that DNx treatment significantly attenuated glomerulosclerosis and interstitial fibrosis at week 10 compared with non-DNx kidneys within the same rats (Figure 8h and i).

DISCUSSION

We observed that renal denervation showed blood pressure control–independent beneficial effects on cardiorenal syndrome accompanied by local RAS inhibition in both the kidney and the heart. Chronic NO inhibition induced local AGT elevations in the heart and kidney with different origins, seemingly circulating AGT in the kidney and cardiac macrophages in the heart, and decreases in renal AGT mRNA

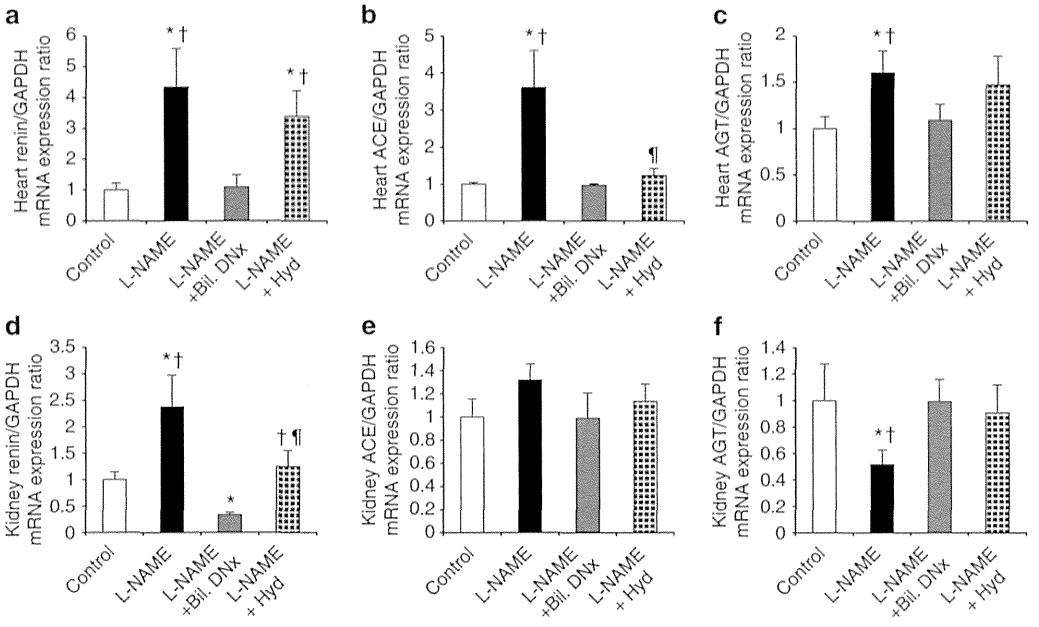

Figure 6 | mRNA expression associated with renin–angiotensin system (RAS) components in the left ventricle and renal cortex in protocol 1. (**a**, **d**) Renin mRNA, (**b**, **e**) ACE mRNA, and (**c**, **f**) AGT mRNA expression levels were analyzed in (**a**–**c**) the left ventricle and (**d**–**f**) renal cortex ($n = 6$–8). Renin mRNA expression levels in the left ventricle were very weak and 400 ng of cDNA was needed to analyze the amplification by real-time PCR. Values are mean ± s.e.m. $^{*}P < 0.05$ vs. control rats, $^{\dagger}P < 0.05$ vs. Bil. DNx rats, $^{\P}P < 0.05$ vs. L-NAME rats. ACE, angiotensin-converting enzyme; AGT, angiotensinogen; Bil. DNx, bilateral renal denervation; GAPDH, glyceraldehyde-3-phosphate dehydrogenase; L-NAME; N^{ω}-nitro-L-arginine methyl ester.

suggested a negative feedback mechanism affected by increases in exogenous AGT inflow into the kidney. We confirmed that the renal sympathetic nerve directly regulated intrarenal RAS and provided renoprotective effects using a unilateral DNx rat model.

Cardiorenal interaction is a multifactorial syndrome involving hemodynamic, neurohumoral, and inflammatory pathways.[34] For neurohumoral factors, interaction between the sympathetic nervous system, RAS, and NO is intricately intertwined and has a crucial role in cardiorenal syndrome.[4,35,36] Sympathetic cross-talk with NO[26,37] and NO–RAS interaction[35] were observed to be closely related. A strength of this study is that the sympathetic nerve–RAS axis was comprehensible to analysis by controlling the interaction between NO and the other two factors by chronic NO inhibition. This chronic L-NAME administration model demonstrates CKD[38,39] and heart failure[40] accompanied by elevations in local[38,40] and circulating[39] RAS and sympathetic overactivity.[41]

In clinical situations of cardiorenal syndrome, many patients demonstrate coexistence of CKD and heart failure with bidirectional organ cross-talk and it is difficult to classify unidirectional mechanisms, these being type 2 and 4 cardiorenal syndrome as devised by Ronco *et al.*[3] Although most experimental studies report observing unidirectional interaction between one insulted organ and the other affected organ,[36] for example, renal changes in heart failure[42] (a type 2 cardiorenal syndrome) or cardiac changes in CKD[43] (a type 4 cardiorenal syndrome), the pathophysiology of cardiorenal syndrome in 'dual-failure' models is poorly understood.[36] The current study is a dual-failure model with bidirectional cardiorenal interaction and is useful for studying the effects of treatment on clinically common cardiorenal syndrome.

Experimental studies of DNx for anti-Thy-1 glomerulonephritis,[44] CKD by subtotal nephrectomy,[45] albuminuria induced by aortic regurgitation,[42] and renal fibrosis in unilateral ureteral obstruction[46] demonstrated mechanisms associated with inflammation,[44,46] oxidative stress,[42,45] and intrarenal RAS.[42] We observed that bilateral DNx, but not unilateral DNx, suppressed cardiorenal interaction, and unilateral DNx showed partial renoprotective effects as a consequence of limited attenuation of intrarenal RAS. These observations indicate that the ipsilateral denervated efferent's effects from the DNx kidney are relatively small, and the contralateral innervated afferent has an important role in the progression of cardiorenal interaction and SNA–RAS overactivity. Questions remain as to why the SYMPLICITY-HTN-3 trial failed to show efficacy.[12] Putting aside discussions about regression to the mean, a placebo effect or the Hawthorne effect, we suggest two most likely reasons: (1) the use of an unsuccessful interventional device; from our own observations of the unilateral DNx model, we noted that incomplete DNx caused blood pressure elevation and organ injury; and (2) inappropriate patient selection for the device; we confirmed DNx did not affect all disease models; for example, DNx did not affect proteinuria and blood pressure in puromycin aminonucleoside nephropathy (data not shown). The current model of NO depletion demonstrated,

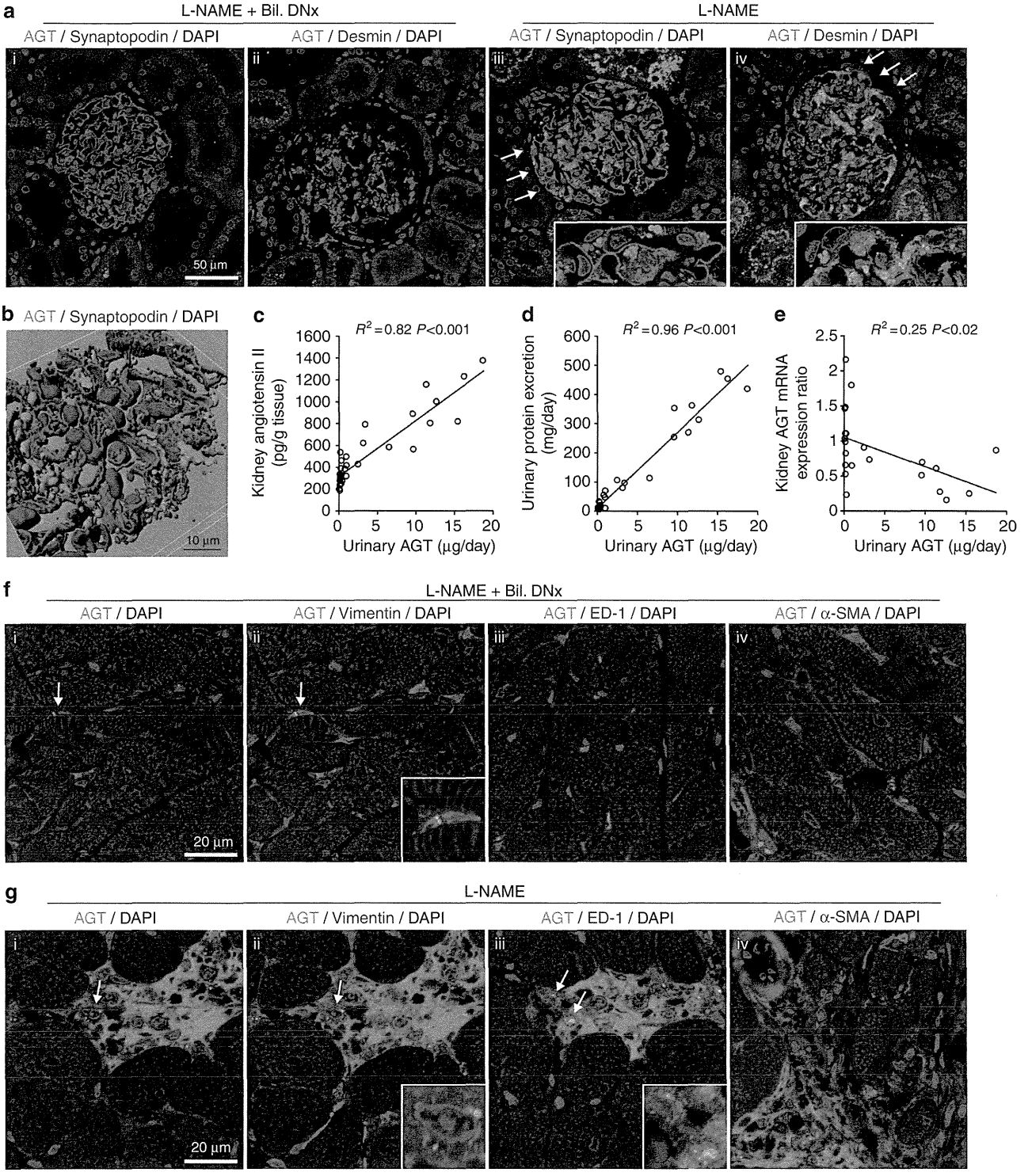

Figure 7 | Angiotensinogen (AGT) protein regulation in the heart and kidney. (**a**) Glomerular immunostaining for AGT, (i, iii) synaptopodin-labeled podocytes, and (ii, iv) desmin-labeled podocytes and mesangial cells. L-NAME induced strong AGT signals in podocytes/mesangial cells (arrows and cropped images; original magnification ×630; water). (**b**) 3D image of L-NAME-induced glomerular injury showed AGT protein was excreted outside the capillary lumen. (**c**–**e**) Association between urinary AGT and kidney angiotensin II, urinary protein, or AGT mRNA in protocol 1. (**f**, **g**) Double staining for AGT and (i, ii) vimentin as a marker of cardiac fibroblasts, macrophages, vascular smooth muscle cells, or pericytes, (iii) ED-1-labeled monocytes/macrophages, or (iv) α-SMA as a label of vascular smooth muscle cells, pericytes, or cardiac myofibroblasts in left ventricle tissue. Arrows and cropped images indicate AGT-producing cells (original magnification ×630; water). Bil. DNx, bilateral renal denervation; DAPI, 4′,6-diamidino-2-phenylindole; GAPDH, glyceraldehyde-3-phosphate dehydrogenase; L-NAME; N^{ω}-nitro-L-arginine methyl ester; α-SMA, α-smooth muscle actin.

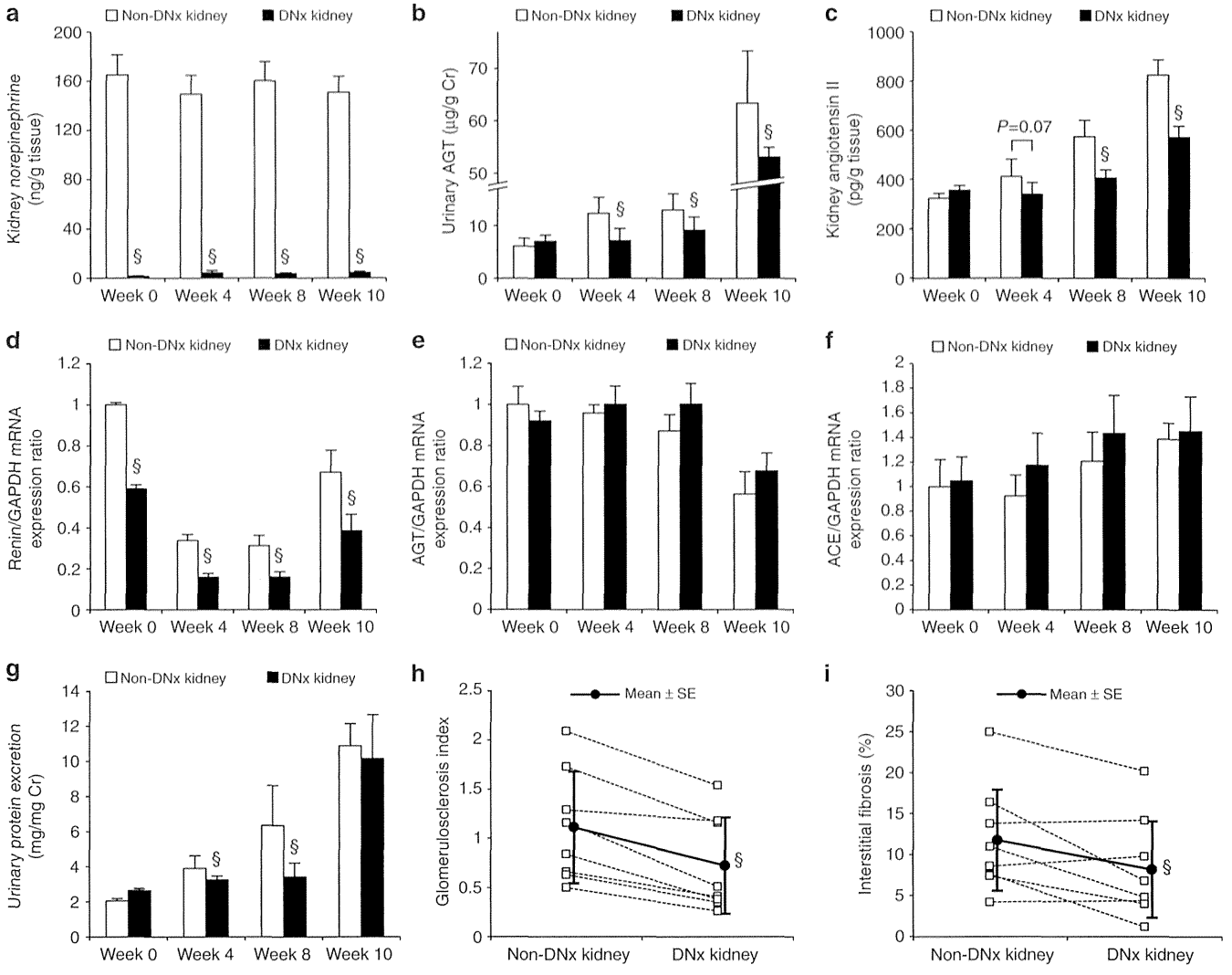

Figure 8 | The validity of renal denervation and protein and mRNA expression of intrarenal renin-angiotensin system (RAS) components and renal injuries in protocol 2. (**a**) Renal cortical norepinephrine content levels were measured to confirm the validity of renal denervation over the study. (**b**) Serial changes in urinary AGT levels from split urine samples. Both ureters were cannulated to collect split urine samples from each DNx and non-DNx kidney. Serial changes in (**c**) renal cortical angiotensin II content levels. Serial changes in renal cortical mRNA expression levels of (**d**) renin, (**e**) AGT, and (**f**) ACE ($n = 6$–8). AGT mRNA levels tended to decrease (P for trend = 0.054) and ACE mRNA tended to increase (P for trend = 0.07) over time. (**g**) Serial changes in urinary protein excretion from DNx and non-DNx kidneys. (**h**) The glomerulosclerosis index at week 10 was assessed as previously described.[38,39] (**i**) Interstitial fibrosis at week 10 using a point-counting technique.[38,39] Further information about kidney weight, urinary volume, urinary creatinine excretion, and creatinine clearance is available in Supplementary Figure S4 online. Values are mean ± s.e.m. $^{\S}P < 0.05$ vs. non-DNx kidney for paired t-tests. ACE, angiotensin-converting enzyme; AGT, angiotensinogen; Cr, creatinine; DNx, renal sympathetic denervation; GAPDH, glyceraldehyde-3-phosphate dehydrogenase; α-SMA, α-smooth muscle actin.

in part, that the renal sympathetic nerve has a critical role in the disruption of blood pressure control and progression of cardiorenal syndrome. Availability of reliable markers to identify and possibly treat patients with DNx is very important and they require to be investigated through further clinical studies.

The mechanisms for increasing local RAS activities are complex, and functional and pathological regulation in the heart[16,28,29,47,48] and kidney[15,17,30,31,33,42] is inconsistent. Several mechanisms, uptake from circulating RAS[30,49] and onsite generation,[15,31,33,42,47,48] and a combination of both,[16,17,29] have been proposed. The complexity of local RAS regulation increases with the many components involved in the generation of AII, such as AGT, renin, ACE, and nonclassical RAS components (cathepsins and chymase), and the possibility that not all components are generated in local tissues—for example, cardiac renin.[28,29] Among current approaches, conditional AGT transgenic models of the heart[27] and kidney,[23,25] but not ACE,[50,51] revealed increases in local AII, indicating that AGT is a rate-limiting factor for local AII generation.[15–17] We examined local RAS generation with a focus on AGT and suggest that intrarenal AGT is caused by increases in proximal tubule uptake of filtered AGT, and cardiac AGT is caused by proliferation of activated

AGT-generating cardiac fibroblasts and macrophages in pathological conditions with chronic NO depletion.

Recently, the origin of AGT in the kidney has been debated. One report suggests that renal AGT is regulated by uptake of liver-origin circulating AGT.[30] Another suggests onsite generation in proximal tubules.[31,33] The results of the current study align with the former mechanism.[30,49] We think that such a result is not inconsistent because local AGT is augmented in many different mechanisms. Chronic plasma AII elevation augments AGT mRNA and protein[33] in the kidney but suppresses it in the heart.[48] Singh *et al.*[47] also reported that beta-adrenergic myocyte stimulation increased AII levels in cells along actin filaments and medium, but high glucose myocyte stimulation increased AII levels only intracellularly in perinuclear and nuclear regions. Different tissues and conditions may involve several mechanisms for local RAS regulation.

From observations of the unilateral denervation model, despite increases in histological renal injury in the non-DNx kidney compared with the contralateral DNx kidney, the non-DNx kidney tended to show increased creatinine clearance compared with that of the contralateral DNx kidney (Supplementary Figure S4c and d online). This may indicate that the glomerular filtration fraction of the non-DNx kidney is greater than that of the contralateral DNx kidney; the non-DNx kidney might represent glomerular hyperfiltration.

A limitation of the current study is that it remains unclear whether renal denervation decreases both proteinuria and urinary AGT as a consequence of decreases in intraglomerular pressure, or whether the renal nerve modulates urinary AGT through other mechanisms—for example, AGT generation in podocytes,[52] glomerular sieving of AGT through slit diaphragm signaling and regulation, and AGT transcytosis across podocytes in the same manner as that previously reported for albumin excretion from podocytes.[53] Although these hypotheses are conjectural, the conditional AGT-KO model may help us further understand the molecular mechanisms.

Another limitation is that the renorenal reflex[13,54,55] was not controlled in protocol 2. The renorenal reflex has a crucial role in balancing total sympathetic nervous activity between kidneys by a negative feedback mechanism.[54,55] Unilateral renal sympathetic denervation with suppression of ipsilateral afferent signals stimulates contralateral renal efferent signals.[54]

With regard to AGT/AII generation in cardiac tissue, cardiac myocytes,[47] fibroblasts,[48] myofibroblasts,[56] and monocyte/macrophages[57,58] have the potential to generate AGT. In the current study, increases in cardiac AGT could be attributed to cardiac fibroblasts and macrophages. Levick *et al.* reported sympathetic modulation of inflammatory cells in the remodeling heart,[59] and we first observed the possibility of renal sympathetic regulation of macrophages associated with local AGT generation in the heart. Further studies are needed to identify specific signaling that connects the renal nerve and cardiac macrophages.

MATERIALS AND METHODS

A detailed methods section is available in the Supplementary Information online.

Ethical considerations

All experimental protocols were performed according to the Ethics Committee on Animal Experimentation, Kyushu University Faculty of Medicine. Eight-week-old male Wistar rats (Kyudo, Saga, Japan) were individually housed in a specific pathogen-free environment on a 12-h day/night cycle and allowed free access to chow containing 2% salt (Oriental Yeast, Tokyo, Japan) and tap water.

Renal denervation

Rats were either bilaterally or unilaterally denervated. Operations were performed 2 days before starting the protocol. DNx was performed as previously described, with slight modification.[42,44–46] The validity of DNx was confirmed by a decrease in norepinephrine content of the denervated kidney to about 5% compared with the innervated kidney. Vehicle-treated and hydralazine-treated rats underwent sham operations.

Experimental protocol 1

Rats were divided into four groups ($n = 8$–10) for a 10-week treatment period. Control rats received untreated drinking water. L-NAME was administered in drinking water (50 mg/kg/day; Sigma, St Louis, MI). L-NAME-treated rats were divided into three groups: (1) vehicle-treated rats; (2) Bil. DNx-treated rats; and (3) hydralazine-treated rats (15 mg/kg/day; Wako Pure Chemical Industries, Osaka, Japan). Tail-cuff pressure was measured in a conscious state using a blood pressure monitor (MK-2000; Muromachi Kikai, Tokyo, Japan) at weeks 0, 4, 8, and 10. Twenty-four-hour urine samples were collected in metabolic cages at weeks 0, 4, 8, and 10. All rats were killed for sample collection at week 10 after echocardiography examination.

Experimental protocol 2

Rats ($n = 32$) received unilateral DNx and L-NAME in drinking water (50 mg/kg/day). Received doses of L-NAME were adjusted as in protocol 1. Groups of eight rats had split urine collection at weeks 0, 4, 8, and 10. Under short-duration anesthesia, bilateral ureters were exposed via bilateral flank incisions and cannulated with a 0.025-inch outer diameter polyurethane tube (MRE025; Braintree Scientific, Braintree, MA) to permit urine collection separately from each ureter. Rats were placed in stabilizers to perform 4-h split urine collection below the level of consciousness. Rats were killed for sample collection after split urine collection.

Echocardiography

Transthoracic echocardiography was performed under anesthesia with sevoflurane with an iU22 (Philips, Andover, MA) equipped with an L15-7io transducer (15 to 7 MHz). Two-dimensional B-mode cine-loops were recorded in mid-papillary short-axis views.

Measurements of RAS components, norepinephrine, and NO metabolite concentrations

Plasma renin activity and AII protein levels were measured by a radioimmunoassay as previously described.[38] AGT protein levels were determined by ELISA (enzyme-linked immunosorbent assay). Norepinephrine concentrations were determined by ELISA and high-performance liquid chromatography. NO metabolite levels in

urine and tissues were quantified with a nitrate/nitrite assay kit (Cayman, Ann Arbor, MI) as previously described.[60]

Histological examination

Kidney and heart tissues embedded in paraffin were used for histological study and immunohistochemistry. Two-micron sections were stained with Masson trichrome, Sirius red, and Periodic acid-Schiff. Degrees of glomerulosclerosis and renal interstitial fibrosis were assessed as previously described.[38,39] Representative histological images were captured using a light microscope (BX53; Olympus, Tokyo, Japan).

Immunohistochemistry

Rat tissues were prepared and stained as previously described, with slight modification,[39] with primary and secondary antibodies as follows: rabbit polyclonal anti-AGT (1:20, IBL); mouse monoclonal anti-desmin (1:100, clone D33, Dako, Glostrup, Denmark); mouse monoclonal anti-synaptopodin (1:200, clone G1D4, Progen, Heidelberg, Germany); mouse monoclonal anti-vimentin (1:50, clone V9, Dako); mouse monoclonal anti-ED-1 (1:500, clone ED-1, Millipore, Billerica, MA); mouse monoclonal anti-α-SMA (1:50, clone 1A4, Abcam, Cambridge, UK); peroxidase-conjugated anti-rabbit (Histofine Simple Stain MAX PO; Nichirei, Tokyo, Japan); Alexa 488-conjugated goat anti-rabbit IgG (1:250, Life Technologies, Carlsbad, CA); and Alexa 568-conjugated goat anti-mouse IgG (1:250, Life Technologies). After counterstaining, representative immunostained images were obtained by light microscopy (BX53; Olympus) or confocal laser scanning microscopy (LSM 710; Carl Zeiss, Oberkochen, Germany) and Z-stack images obtained by LSM 710 were reconstructed to three-dimensional images by image analyzing software (Imaris; Bitplane, Belfast, UK).

Western blot analysis

Protein samples (15 mg) were separated on SDS–PAGE and blotted onto a polyvinylidene difluoride membrane using an iBlot system (Life Technologies). Immunoreactive bands were detected with rabbit polyclonal anti-AGT (1:100, IBL, Fujioka, Japan), rabbit polyclonal anti-β-actin (1:2000, Abcam), and mouse monoclonal anti-glyceraldehyde-3-phosphate dehydrogenase (GAPDH) (1:2000, Clone 6C5, Abcam). The density of each band was analyzed using a chemiluminescence imaging system (AE-9300 Ez-capture MG; Atto, Tokyo, Japan).

Real-time PCR

Total RNA was extracted from the tissue and complementary DNA was synthesized. Using SYBR Premix Ex Taq (Takara Bio, Otsu, Japan) and Applied Biosystems 7500 Real-Time PCR Systems (Applied Biosystems, Foster, CA), real-time PCR was performed. Relative amounts for renin, ACE, AGT, AII type 1a receptor, brain natriuretic peptide, transforming growth factor-β1, osteopontin, platelet-derived growth factor-BB, and collagen I were determined by the relative standard curve method using GAPDH as an internal reference.

Statistical analyses

Statistical analyses were performed using SPSS version 19.0 software (IBM, Armonk, NY). Results are presented as mean ± s.e.m. Differences among groups were compared by one-way ANOVA (analysis of variance), followed by Tukey's honestly significant difference tests. Sequential repeated measurement values were analyzed using two-way repeated measures ANOVA followed by Dunnett's tests for differences from baseline values. A paired t-test was used for comparisons of paired values within the same rats. Linear trends in serial mean values over time in protocol 2 were tested using linear regression analysis. For all tests, a two-tailed P-value < 0.05 was considered statistically significant.

DISCLOSURE

The authors declare that they have no conflict of interest and received no financial support from any source including any marketer or shareholder associated with catheter-based DNx.

ACKNOWLEDGMENTS

We thank Dr Tomoyuki Tobushi and Dr Tomomi Ide at the Department of Cardiovascular Medicine, Graduate School of Medical Sciences, Kyushu University, for their helpful assistance in performing the echocardiography. We also thank Dr Masayo Fukuhara and Dr Kiyoshi Matsumura at the Department of Medicine and Clinical Science, Graduate School of Medical Sciences, Kyushu University, for their helpful assistance in performing renal denervation. We also appreciate the technical support of the Research Support Center, Graduate School of Medical Sciences, Kyushu University.

SUPPLEMENTARY MATERIAL

Figure S1. AGT protein and mRNA expression in the liver.
Figure S2. Other mRNA expression in the renal cortex.
Figure S3. Other mRNA expression in the left ventricle.
Figure S4. Other split renal function in protocol 2.
Table S1. Clinical parameters in protocol 1.
Table S2. Echocardiographic data at week 10 in protocol 1.
Table S3. Clinical parameters in protocol 2.
Supplementary material is linked to the online version of the paper at http://www.nature.com/ki

REFERENCES

1. Weiner DE, Tighiouart H, Amin MG *et al.* Chronic kidney disease as a risk factor for cardiovascular disease and all-cause mortality: a pooled analysis of community-based studies. *J Am Soc Nephrol* 2004; **15**: 1307–1315.
2. Forman DE, Butler J, Wang Y *et al.* Incidence, predictors at admission, and impact of worsening renal function among patients hospitalized with heart failure. *J Am Coll Cardiol* 2004; **43**: 61–67.
3. Ronco C, Haapio M, House AA *et al.* Cardiorenal syndrome. *J Am Coll Cardiol* 2008; **52**: 1527–1539.
4. Bongartz LG, Cramer MJ, Doevendans PA *et al.* The severe cardiorenal syndrome: 'Guyton revisited'. *Eur Heart J* 2005; **26**: 11–17.
5. Krum H, Schlaich M, Whitbourn R *et al.* Catheter-based renal sympathetic denervation for resistant hypertension: a multicentre safety and proof-of-principle cohort study. *Lancet* 2009; **373**: 1275–1281.
6. Brandt MC, Mahfoud F, Reda S *et al.* Renal sympathetic denervation reduces left ventricular hypertrophy and improves cardiac function in patients with resistant hypertension. *J Am Coll Cardiol* 2012; **59**: 901–909.
7. Mahfoud F, Cremers B, Janker J *et al.* Renal hemodynamics and renal function after catheter-based renal sympathetic denervation in patients with resistant hypertension. *Hypertension* 2012; **60**: 419–424.
8. Mahfoud F, Schlaich M, Kindermann I *et al.* Effect of renal sympathetic denervation on glucose metabolism in patients with resistant hypertension: a pilot study. *Circulation* 2011; **123**: 1940–1946.
9. Witkowski A, Prejbisz A, Florczak E *et al.* Effects of renal sympathetic denervation on blood pressure, sleep apnea course, and glycemic control in patients with resistant hypertension and sleep apnea. *Hypertension* 2011; **58**: 559–565.
10. Brandt MC, Reda S, Mahfoud F *et al.* Effects of renal sympathetic denervation on arterial stiffness and central hemodynamics in patients with resistant hypertension. *J Am Coll Cardiol* 2012; **60**: 1956–1965.
11. Hering D, Mahfoud F, Walton AS *et al.* Renal denervation in moderate to severe CKD. *J Am Soc Nephrol* 2012; **23**: 1250–1257.
12. Bhatt DL, Kandzari DE, O'Neill WW *et al.* A controlled trial of renal denervation for resistant hypertension. *N Engl J Med* 2014; **370**: 1393–1401.
13. Jordan J, Mann JF, Luft FC. Research needs in the area of device-related treatments for hypertension. *Kidney Int* 2013; **84**: 250–255.

14. Paul M, Poyan Mehr A, Kreutz R. Physiology of local renin-angiotensin systems. *Physiol Rev* 2006; **86**: 747–803.
15. Kobori H, Nangaku M, Navar LG *et al.* The intrarenal renin-angiotensin system: from physiology to the pathobiology of hypertension and kidney disease. *Pharmacol Rev* 2007; **59**: 251–287.
16. Dostal DE, Baker KM. The cardiac renin-angiotensin system: conceptual, or a regulator of cardiac function? *Circ Res* 1999; **85**: 643–650.
17. Lu X, Roksnoer LC, Danser AH. The intrarenal renin-angiotensin system: does it exist? Implications from a recent study in renal angiotensin-converting enzyme knockout mice. *Nephrol Dial Transplant* 2013; **28**: 2977–2982.
18. Levens NR, Peach MJ, Carey RM. Role of the intrarenal renin-angiotensin system in the control of renal function. *Circ Res* 1981; **48**: 157–167.
19. Ellis B, Li XC, Miguel-Qin E *et al.* Evidence for a functional intracellular angiotensin system in the proximal tubule of the kidney. *Am J Physiol Regul Integr Comp Physiol* 2012; **302**: R494–R509.
20. Sakai K, Agassandian K, Morimoto S *et al.* Local production of angiotensin II in the subfornical organ causes elevated drinking. *J Clin Invest* 2007; **117**: 1088–1095.
21. Schinke M, Baltatu O, Bohm M *et al.* Blood pressure reduction and diabetes insipidus in transgenic rats deficient in brain angiotensinogen. *Proc Natl Acad Sci USA* 1999; **96**: 3975–3980.
22. Lindpaintner K, Ganten D. The cardiac renin-angiotensin system. An appraisal of present experimental and clinical evidence. *Circ Res* 1991; **68**: 905–921.
23. Sachetelli S, Liu Q, Zhang SL *et al.* RAS blockade decreases blood pressure and proteinuria in transgenic mice overexpressing rat angiotensinogen gene in the kidney. *Kidney Int* 2006; **69**: 1016–1023.
24. Yamamoto T, Nakagawa T, Suzuki H *et al.* Urinary angiotensinogen as a marker of intrarenal angiotensin II activity associated with deterioration of renal function in patients with chronic kidney disease. *J Am Soc Nephrol* 2007; **18**: 1558–1565.
25. Kobori H, Ozawa Y, Satou R *et al.* Kidney-specific enhancement of ANG II stimulates endogenous intrarenal angiotensinogen in gene-targeted mice. *Am J Physiol Renal Physiol* 2007; **293**: F938–F945.
26. Campese VM, Ye S, Zhong H. Downregulation of neuronal nitric oxide synthase and interleukin-1beta mediates angiotensin II-dependent stimulation of sympathetic nerve activity. *Hypertension* 2002; **39**: 519–524.
27. Domenighetti AA, Wang Q, Egger M *et al.* Angiotensin II-mediated phenotypic cardiomyocyte remodeling leads to age-dependent cardiac dysfunction and failure. *Hypertension* 2005; **46**: 426–432.
28. Dzau VJ, Re R. Tissue angiotensin system in cardiovascular medicine. A paradigm shift? *Circulation* 1994; **89**: 493–498.
29. Kumar R, Singh VP, Baker KM. The intracellular renin-angiotensin system: a new paradigm. *Trends Endocrinol Metab* 2007; **18**: 208–214.
30. Matsusaka T, Niimura F, Pastan I *et al.* Podocyte injury enhances filtration of liver-derived angiotensinogen and renal angiotensin II generation. *Kidney Int* 2013; **85**: 1068–1077.
31. Nakano D, Kobori H, Burford JL *et al.* Multiphoton imaging of the glomerular permeability of angiotensinogen. *J Am Soc Nephrol* 2012; **23**: 1847–1856.
32. Kobori H, Harrison-Bernard LM, Navar LG. Urinary excretion of angiotensinogen reflects intrarenal angiotensinogen production. *Kidney Int* 2002; **61**: 579–585.
33. Kobori H, Harrison-Bernard LM, Navar LG. Expression of angiotensinogen mRNA and protein in angiotensin II-dependent hypertension. *J Am Soc Nephrol* 2001; **12**: 431–439.
34. Palazzuoli A, Ronco C. Cardio-renal syndrome: an entity cardiologists and nephrologists should be dealing with collegially. *Heart Fail Rev* 2011; **16**: 503–508.
35. Kopkan L, Cervenka L. Renal interactions of renin-angiotensin system, nitric oxide and superoxide anion: implications in the pathophysiology of salt-sensitivity and hypertension. *Physiol Res* 2009; **58**(Suppl 2): S55–S67.
36. Bongartz LG, Braam B, Gaillard CA *et al.* Target organ cross talk in cardiorenal syndrome: animal models. *Am J Physiol Renal Physiol* 2012; **303**: F1253–F1263.
37. Shabeeh H, Seddon M, Brett S *et al.* Sympathetic activation increases NO release from eNOS but neither eNOS nor nNOS play an essential role in exercise hyperemia in the human forearm. *Am J Physiol Heart Circ Physiol* 2013; **304**: H1225–H1230.
38. Kashiwagi M, Shinozaki M, Hirakata H *et al.* Locally activated renin-angiotensin system associated with TGF-beta1 as a major factor for renal injury induced by chronic inhibition of nitric oxide synthase in rats. *J Am Soc Nephrol* 2000; **11**: 616–624.
39. Ikeda H, Tsuruya K, Toyonaga J *et al.* Spironolactone suppresses inflammation and prevents L-NAME-induced renal injury in rats. *Kidney Int* 2009; **75**: 147–155.
40. Takemoto M, Egashira K, Usui M *et al.* Important role of tissue angiotensin-converting enzyme activity in the pathogenesis of coronary vascular and myocardial structural changes induced by long-term blockade of nitric oxide synthesis in rats. *J Clin Invest* 1997; **99**: 278–287.
41. Sakuma I, Togashi H, Yoshioka M *et al.* NG-methyl-L-arginine, an inhibitor of L-arginine-derived nitric oxide synthesis, stimulates renal sympathetic nerve activity in vivo. A role for nitric oxide in the central regulation of sympathetic tone? *Circ Res* 1992; **70**: 607–611.
42. Rafiq K, Noma T, Fujisawa Y *et al.* Renal sympathetic denervation suppresses de novo podocyte injury and albuminuria in rats with aortic regurgitation. *Circulation* 2012; **125**: 1402–1413.
43. Rabkin R, Awwad I, Chen Y *et al.* Low-dose growth hormone is cardioprotective in uremia. *J Am Soc Nephrol* 2008; **19**: 1774–1783.
44. Veelken R, Vogel EM, Hilgers K *et al.* Autonomic renal denervation ameliorates experimental glomerulonephritis. *J Am Soc Nephrol* 2008; **19**: 1371–1378.
45. Nagasu H, Satoh M, Kuwabara A *et al.* Renal denervation reduces glomerular injury by suppressing NAD(P)H oxidase activity in Dahl salt-sensitive rats. *Nephrol Dial Transplant* 2010; **25**: 2889–2898.
46. Kim J, Padanilam BJ. Renal nerves drive interstitial fibrogenesis in obstructive nephropathy. *J Am Soc Nephrol* 2013; **24**: 229–242.
47. Singh VP, Le B, Bhat VB *et al.* High-glucose-induced regulation of intracellular ANG II synthesis and nuclear redistribution in cardiac myocytes. *Am J Physiol Heart Circ Physiol* 2007; **293**: H939–H948.
48. Dostal DE, Booz GW, Baker KM. Regulation of angiotensinogen gene expression and protein in neonatal rat cardiac fibroblasts by glucocorticoid and beta-adrenergic stimulation. *Basic Res Cardiol* 2000; **95**: 485–490.
49. Pohl M, Kaminski H, Castrop H *et al.* Intrarenal renin angiotensin system revisited: role of megalin-dependent endocytosis along the proximal nephron. *J Biol Chem* 2010; **285**: 41935–41946.
50. Tian XL, Pinto YM, Costerousse O *et al.* Over-expression of angiotensin converting enzyme-1 augments cardiac hypertrophy in transgenic rats. *Hum Mol Genet* 2004; **13**: 1441–1450.
51. Gonzalez-Villalobos RA, Janjoulia T, Fletcher NK *et al.* The absence of intrarenal ACE protects against hypertension. *J Clin Invest* 2013; **123**: 2011–2023.
52. Yoo TH, Li JJ, Kim JJ *et al.* Activation of the renin-angiotensin system within podocytes in diabetes. *Kidney Int* 2007; **71**: 1019–1027.
53. Kinugasa S, Tojo A, Sakai T *et al.* Selective albuminuria via podocyte albumin transport in puromycin nephrotic rats is attenuated by an inhibitor of NADPH oxidase. *Kidney Int* 2011; **80**: 1328–1338.
54. Colindres RE, Spielman WS, Moss NG *et al.* Functional evidence for renorenal reflexes in the rat. *Am J Physiol* 1980; **239**: F265–F270.
55. Kopp UC, Smith LA, DiBona GF. Renorenal reflexes: neural components of ipsilateral and contralateral renal responses. *Am J Physiol* 1985; **249**: F507–F517.
56. Katwa LC, Campbell SE, Tyagi SC *et al.* Cultured myofibroblasts generate angiotensin peptides de novo. *J Mol Cell Cardiol* 1997; **29**: 1375–1386.
57. Kitazono T, Padgett RC, Armstrong ML *et al.* Evidence that angiotensin II is present in human monocytes. *Circulation* 1995; **91**: 1129–1134.
58. Gomez RA, Norling LL, Wilfong N *et al.* Leukocytes synthesize angiotensinogen. *Hypertension* 1993; **21**: 470–475.
59. Levick SP, Murray DB, Janicki JS *et al.* Sympathetic nervous system modulation of inflammation and remodeling in the hypertensive heart. *Hypertension* 2010; **55**: 270–276.
60. Miyazawa T, Zeng F, Wang S *et al.* Low nitric oxide bioavailability upregulates renal heparin binding EGF-like growth factor expression. *Kidney Int* 2013; **84**: 1176–1188.

Therapeutic Apheresis and Dialysis

Therapeutic Apheresis and Dialysis 2015; 19(1):73–80
doi: 10.1111/1744-9987.12221

Fibroblast Growth Factor 23, but not Parathyroid Hormone, Is Associated With Urinary Phosphate Regulation in Patients on Peritoneal Dialysis

Shunsuke Yamada,[1,3] Kazuhiko Tsuruya,[1,2] Masanori Tokumoto,[3] Hisako Yoshida,[2] Shoko Hasegawa,[1] Shigeru Tanaka,[1] Masahiro Eriguchi,[1] Toshiaki Nakano,[1] Kosuke Masutani,[1] Hiroaki Ooboshi,[3] and Takanari Kitazono[1]

[1]Department of Medicine and Clinical Science, Graduate School of Medical Sciences, [2]Department of Integrated Therapy for Chronic Kidney Disease, Graduate School of Medical Sciences, Kyushu University, and [3]Division of Internal Medicine, Fukuoka Dental College, Fukuoka, Japan

Abstract: Fibroblast growth factor (FGF) 23 plays an important role in regulation of renal phosphate excretion in patients with chronic kidney disease. However, it remains undetermined whether FGF23 is closely linked to renal phosphate handling in patients with low glomerular filtration rate (GFR). The present cross-sectional study included 52 outpatients undergoing peritoneal dialysis with urine volume ≥ 100 mL/day. The primary outcome was level of urinary phosphate excretion, and the secondary outcomes were tubular maximal reabsorption of phosphate normalized to GFR (TmP/GFR), an index of the renal threshold for phosphate excretion, and level of peritoneal phosphate excretion. Variates of interest were serum FGF23 and parathyroid hormone (PTH) levels. The median and interquartile range of serum FGF23 level, TmP/GFR, and total urinary and peritoneal phosphate excretion were 5610 (1493–11 430) ng/mL, 1.30 (0.44–1.86) mg/dL, 117 (40–234) mg/day, and 208 (156–250) mg/day, respectively. Multivariate linear regression analysis revealed that serum FGF23 level was significantly ($P < 0.05$) associated with TmP/GFR negatively and significantly ($P < 0.05$) associated with urinary phosphate excretion positively, even after adjusting for confounders. In contrast, none of the three outcome variates was associated with serum PTH level. Neither serum FGF23 nor PTH level was associated with peritoneal phosphate excretion. The present study indicates that FGF23, but not PTH, is involved in urinary phosphate regulation, even in patients on peritoneal dialysis with residual renal function. **Key Words:** Fibroblast growth factor 23, Parathyroid hormone, Peritoneal dialysis, Residual renal function, Urinary phosphate excretion.

The prevalence of relative inorganic phosphate (Pi) overload, as demonstrated by hyperphosphatemia, increases as the residual renal function (RRF) declines in patients undergoing peritoneal dialysis (PD) (1–3). Urinary Pi excretion is primarily regulated by the expression of the Na–Pi co-transporters type II on the apical side of the renal proximal tubules (4). The Na–Pi co-transporters are principally regulated by parathyroid hormone (PTH) and fibroblast growth factor (FGF) 23 (5). When the serum PTH and FGF23 levels increase, the expression of Na–Pi type II in the proximal tubules is down-regulated, leading to a decrease in the tubular reabsorption rate of Pi and a resultant increase in urinary Pi excretion (6). In patients with chronic kidney disease (CKD), both the serum FGF23 and PTH levels begin to increase as early as CKD stage 2 and 3 (7), stimulating a compensatory increase in urinary Pi excretion and achieving a normal serum Pi level in the early stage of CKD.

The prevalence of overt hyperphosphatemia increases as the stage of CKD progresses (7,8). These results indicate that the phosphaturic effects of both FGF23 and PTH are no longer sufficient to maintain Pi homeostasis in the late CKD stage. Several clinical studies have already investigated the association

Received February 2014; revised April 2014.
Address correspondence and reprint requests to Dr Kazuhiko Tsuruya, Department of Integrated Therapy for Chronic Kidney Disease, Graduate School of Medical Sciences, Kyushu University, Maidashi3-1-1, Higashi-ku, Fukuoka 812-8582, Japan. Email: tsuruya@intmed2.med.kyushu-u.ac.jp

between these hormones and urinary Pi excretion in post-transplant CKD patients and peritoneal dialysis patients (9,10). However, it remains undetermined whether FGF23 and PTH exert their phosphaturic effect in patients with such decreased kidney function as well as in PD patients.

Our main goal was to establish whether the serum levels of FGF23 and PTH were closely linked to urinary Pi excretion in patients with decreased kidney function. We examined the association between these two hormones and daily urinary Pi excretion and/or tubular maximal reabsorption of Pi normalized to glomerular filtration rate (TmP/GFR) in PD patients with residual renal function (RRF). Serum levels of various markers including FGF23 and PTH are more stable in PD than in hemodialysis patients. PD patients are suitable targets for determining the association between serum markers.

PATIENTS AND METHODS

Study design and participants

This single-center cross-sectional study included 60 prevalent outpatients who received PD at Kyushu University Hospital between September 2010 and April 2012. The present study was designed to investigate the correlation between the levels of serum phosphaturic hormones (FGF23 and PTH) and urinary and peritoneal Pi excretion. The primary outcome variate was urinary Pi excretion. The secondary outcome variates were TmP/GFR and peritoneal Pi excretion. Covariates of interest were serum FGF23 and PTH levels. Four patients who did not undergo measurement of serum intact FGF23 levels were excluded. Another four patients with urine volume <100 mL/day were excluded, because we defined patients with urine volume ≥100 mL/day as having RRF. The remaining 52 patients were enrolled in the present analysis.

The study protocol was approved by the local Ethics Committee of Kyushu University Hospital (No. 24–56) and registered in the Clinical Trial Registry (UMIN000009315). This study was performed according to the Ethics of Clinical Research (Declaration of Helsinki). Written informed consent was obtained from each patient prior to study participation.

Data collection

Blood samples and 24-h urine and peritoneal dialysates were simultaneously collected in the morning with fasting at each 6-month examination. Demographic and clinical data at the time of each regular visit were also recorded. In the present study, calcium carbonate, sevelamer hydrochloride, and lanthanum carbonate were used as Pi binders, and alfacalcidol and calcitriol were used as vitamin D receptor activators. No patients underwent parathyroidectomy at the time of entry. Samples of blood, urine, and peritoneal dialysate were centrifuged at room temperature and stored at −80°C until analysis.

Measurement of biochemical parameters

The levels of urea nitrogen, creatinine (Cr), albumin, Pi, and corrected Ca in the serum, urine, and peritoneal dialysate were measured according to standard procedures (11). Enzyme-linked immunosorbent assay kits were used to measure the serum levels of intact FGF23 (Kainos Laboratories, Tokyo, Japan) and whole PTH (Scantibodies Laboratory, Santee, CA, USA) (12,13).

Calculation of outcome variates and indexes

As an index of renal threshold for Pi, we calculated TmP/GFR instead of the fractional excretion of Pi based on previous reports, because TmP/GFR is more independent of GFR and serum Pi level, and is useful when GFR is low (9,14,15). GFR was calculated by the arithmetic mean of urea clearance and Cr clearance (16). Estimated Pi intake was calculated based on the normalized protein catabolic rate: estimated Pi intake (mg/day) = normalized protein catabolic rate (g/kg per day) × body weight (kg) × 15 (mg/g) (17). Kt/V for urea, Cr clearance, and D/P Cr at 4 h were calculated by standard methods (16).

Statistical analysis

The results are expressed as the mean (standard deviation) for variates with a normal distribution, the median (interquartile range) for variates with a skewed distribution, and the frequency (percentage) for categorical variates, as appropriate. In the present study, the variates of interest were serum intact FGF23 and whole PTH levels. Urinary and peritoneal Pi excretion and serum levels of intact FGF23 and whole PTH were transformed into logarithms to improve the skewed distributions. Differences between the two groups were compared using unpaired *t*-tests for parametric variates, Wilcoxon's signed-rank test for skewed distribution, and the χ^2 test for categorical variates. Linear regression analyses were used to assess the associations between serum intact FGF23 and whole PTH levels, and TmP/GFR and total urinary and peritoneal Pi excretion. Variates that exhibited a *P*-value <0.1 in the univariate analysis were included in the multivariate linear regression analysis. A two-tailed *P*-value <0.05 was

considered to be statistically significant. All statistical analyses were conducted using the JMP 10.0 software program (SAS Institute, Tokyo, Japan).

RESULTS

Patient characteristics

A total of 52 PD patients were included in the present analysis. A summary of the patients' baseline characteristics is provided in Table 1. The mean patient age was 56 ± 13 years. A total of 34 patients (65%) were male and 15 (29%) had diabetes mellitus. The median and interquartile range of dialysis vintage was 541 (24–980) days. The serum Cr level was 839 ± 274 μmol/L, serum corrected Ca level was 2.37 ± 0.13 mmol/L, and serum Pi level was 1.65 ± 0.36 mmol/L. Serum FGF23 level, serum whole PTH, TmP/GFR, and total urinary and peritoneal Pi excretion were 5610 (1493–11 430) pg/mL, 74 (48–146) pg/mL, 1.30 (0.44–1.86) mg/dL, 117 (40–234) mg/day, and 208 (156–250) mg/day, respectively. Eight patients (15%) used cinacalcet and 25 (48%) used vitamin D receptor activators.

Relationship between phosphaturic hormones, TmP/GFR and total urinary Pi excretion

Linear regression analyses showed log serum FGF23 to be negatively and significantly associated with TmP/GFR, but positively with log urinary Pi excretion, while log serum whole PTH was associated

TABLE 1. *Patient characteristics*

Variate	Value
Age, years	56 ± 13
Sex (male), *N* (%)	34 (65)
Underlying kidney disease	
Diabetes mellitus, *N* (%)	15 (29)
Dialysis vintage, day	541 (24, 980)
Body mass index, kg/m^2	22.4 ± 3.0
nPCR, g/kg per day	0.94 ± 0.23
Serum biochemistry	
Albumin, g/L	34 ± 5
Urea nitrogen, mmol/L	23.3 ± 5.3
Creatinine, μmol/L	839 ± 274
Corrected calcium, mmol/L	2.37 ± 0.13
Pi, mmol/L	1.65 ± 0.36
Whole PTH, pg/mL	74 (48,146)
FGF23, pg/mL	5610 (1493, 11430)
Parameters related to residual renal function and PD	
Urine volume, mL/day	750 (420, 1238)
Dialysate volume, mL/day	6000 (4500, 8300)
Peritoneal ultrafiltration volume, mL/day	400 (11, 712)
Renal creatinine clearance, L/week	34.4 (13.6, 54.5)
Renal creatinine clearance, mL/min per 1.73 m^2	3.00 (0.75, 4.55)
Peritoneal creatinine clearance, L/week	34.7 (26.1, 40.2)
Renal Kt/V for urea	0.494 (0.286, 0.765)
Peritoneal Kt/V for urea	1.128 (0.932, 1.305)
Use of automated peritoneal dialysis, *N* (%)	26 (50)
D/P creatinine at 4 h	0.70 ± 0.15
Pi homeostasis related parameters	
Urinary Pi excretion, mg/day	117 (40, 234)
Peritoneal Pi excretion, mg/day	208 (156, 250)
Estimated Pi intake, mg/day	818 (673, 947)
TmP/GFR	1.30 (0.44, 1.86)
Drug prescription	
Use of Pi-binder, *N* (%)	41 (79)
Use of vitamin D receptor activator, n (%)	25 (48)
Use of cinacalcet, *N* (%)	8 (15)

Data for 52 patients. The data are presented as the mean ± standard deviation, median (25 percentile, 75 percentile) or number (percentage) of patients. D/P creatinine, dialysis creatinine concentration per peritoneal creatinine concentration; FGF23, fibroblast growth factor 23; Kt/V for urea, dialysis adequacy; nPCR, normalized protein catabolic rate; PD, peritoneal dialysis; Pi, phosphate; PTH, parathyroid hormone; TmP/GFR, tubular maximal Pi reabsorption normalized to glomerular filtration rate.